MODELLING OF POWER GENERATION FROM THERMOELECTRIC CELLS BY USING A SOLAR TROUGH CONCENTRATOR SYSTEM

2023
PhD THESIS
ENERGY SYSTEMS ENGİNEERİNG

Abdalhakim BEN SAOUD

Thesis Advisor
Assoc. Prof. Dr. Engin GEDİK

MODELLING OF POWER GENERATION FROM THERMOELECTRIC CELLS BY USING A SOLAR TROUGH CONCENTRATOR SYSTEM

Abdalhakim BEN SAOUD

Thesis Advisor

Assoc. Prof. Dr. Engin GEDİK

T.C.

Karabuk University

Institute of Graduate Programs

Department of Energy Systems Engineering

Prepared as

PhD Thesis

KARABUK

February 2023

I certify that in my opinion the thesis submitted by Abdalhakim BEN SAOUD titled "MODELLING OF POWER GENERATION FROM THERMOELECTRIC CELLS BY USING A SOLAR TROUGH CONCENTRATOR SYSTEM" is fully adequate in scope and in quality as a thesis for the degree of PhD.

Assoc. Prof. Dr. Engin GEDİK .....
Thesis Advisor, Department of Energy Systems Engineering

This thesis is accepted by the examining committee with a unanimous vote in the Department of Energy Systems Engineering as a PhD thesis. 23/02/2023

Examining Committee Members (Institutions)	Signature
Chairman : Prof. Dr. Mehmet OZKAYMAK (KBU)	.....
Member : Prof. Dr. Kamil ARSLAN (KBU)	.....
Member : Prof. Dr. Ali KECEBAS (MU)	.....
Member : Prof. Dr. Mustafa AKTAS (GU)	.....
Member : Assoc. Prof. Dr. Engin GEDİK (KBU)	.....

The degree of PhD by the thesis submitted is approved by the Administrative Board of the Institute of Graduate Programs, Karabuk University.

Prof. Dr. Müslüm KUZU .....
Director of the Institute of Graduate Programs

"I declare that all the information within this thesis has been gathered and presented in accordance with academic regulations and ethical principles and I have according to the requirements of these regulations and principles cited all those which do not originate in this work as well."

Abdalhakim Faitori BEN SAOUD

ABSTRACT

PhD. Thesis

MODELLING OF POWER GENERATION FROM THERMOELECTRIC CELLS BY USING A SOLAR TROUGH CONCENTRATOR SYSTEM

Abdalhakim Faitori BEN SAOUD

Karabük University
Institute of Graduate Programs
Department of Energy Systems Engineering

Thesis Advisor:
Assoc. Prof. Dr. Engin GEDİK
February 2023, 72 pages

The solar thermoelectric generators (STEGs) have emerged during the past decade as a promising substitutional among other green power production systems. Recent developments in solar thermoelectric generator have achieved several improvements as a result of its optimized systems such as concentrated systems and also the boosts from nanotechnology. In this study, a concentrator thermoelectric generator (CTEG) using Graphene Nanoplatelets (GNPs), Multiwall Carbon Nanotubes (MWCNTs) dispersed in water and distilled water as base fluid was investigated experimentally. The CTEG system was designed and constructed in Karabuk university labs, Turkey and have been commissioned outdoor by testing, balancing, and adjusting. Experiments were performed for 0.25 wt.% and 0.50wt% nanoparticle mass concentration of MWCNTs-distilled water, GNPs-distilled water nanofluids and distilled water with a constant volume rate of flow ($\dot{v}$=0.5 L/min). Experiments study aimed to study effect of nanoparticle types on thermal and electrical

efficiencies. The obtained results showed that the CTEG is enabled to generate (E_{max}=3.7 W) of electrical power output for an average temperature difference of 38°C. MWCNTs- distilled water nanofluid presented an enhancement in electrical performance more than GNPs- distilled water nanofluid and distilled water, while GNPs-distilled water nanofluid presented maximum thermal increasement. The total efficiency for the day-long periods were 18.69%, 19.87% and 18.91% for distilled water, GNPs-distilled water, MWCNTs-distilled water respectively. The results of the study made a solid basics about the prospects of CTEG applications related with nanotechnology to be one of the potential choices for cooling technique by using different types of nanofluids as coolants.

Keywords : Solar Energy, Concentrator Thermoelectric Generator (CTEG), Thermoelectric modules, Nanofluids, Cooling technique

Science Code : 92802

ÖZET

Doktora Tezi

TERMOELEKTRİK HÜCRELERDEN ELEKTRİK ÜRETİMİNİN GÜNEŞ OLUKLU YOĞUNLUK SİSTEMİ KULLANARAK MODELLENMESİ

Abdalhakim Faitori BEN SAOUD

Karabük Üniversitesi
Lisansüstü Eğitim Enstitüsü
Enerji Sistemleri Mühendisliği Anabilim Dalı

Tez Danışmanları:
Doç. Dr. Engin GEDİK
Şubat 2023, 72 sayfa

Güneş termoelektrik jeneratörleri (GTJ), son on yılda diğer yeşil enerji üretim sistemleri arasında yer almaktadır. Güneş termoelektrik jeneratöründeki son gelişmeler, konsantre sistemler gibi optimize edilmiş sistemlerin ve ayrıca nanoteknolojiden gelen desteklerin bir sonucu olarak çeşitli iyileştirmeler sağlamıştır. Bu çalışmada, baz akışkan olarak kullanılan saf suda dağıtılmış Grafen nanoplatet'ler (GNP) ve çok duvarlı karbon nanotüpler (MWCNT) bir yoğunlaştırıcı termoelektrik jeneratöründe kullanılmış ve deneysel olarak incelenmiştir. Deney düzeneği Karabük Üniversitesi laboratuvarlarında tasarlanmış ayarlama yapılarak açık havada devreye alınmıştır. Deneyler, sabit hacim akış hızına sahip ($\dot{v}$=0,5 L/dk) MWCNT/saf su ve GNP-saf su nanoakışkanlarının ağırlıkça %0,25 ve %0,50 nanoparçacık kütle konsantrasyonunda gerçekleştirilmiştir. Çalışmada, nanoparçacık türlerinin termal ve elektriksel enerji verimliliği üzerindeki etkisi incelemek amaçlanmıştır. Elde edilen sonuçlar ışığında ortalama 38°C'lik bir sıcaklık farkı için

(Emax=3.7 W) elektrik gücü çıkışı üretebildiğini göstermektedir. MWCNT- saf su nanoakışkanı, GNP-saf su nanoakışkanı saf suya kıyasla daha fazla elektriksel performans artışı sunarken, GNP-saf su nanoakışkanı maksimum termal artış göstermektedir. Gün boyu süreler için toplam verimlilik, saf su, GNP-saf su ve MWCNT-saf su için sırasıyla %18,69 , %19,87 ve %18,91 hesaplanmıştır. Çalışmanın sonuçları, nanoteknoloji ile ilgili yoğunlaştırıcı güneş termoelektrik uygulamalarının, soğutucu olarak farklı türde nanoakışkanlar kullanarak soğutma tekniği için potansiyel seçeneklerden biri olma beklentilerini karşılamaktadır.

Anahtar Kelimeler: Güneş Enerjisi, Yoğunlaştıcılı Termoelektrik Üretici, Termoelektrik modüller, Nanoakışkanlar, Soğutma Tekniği.

Bilim Kodu **:** 92802

ACKNOWLEDGMENT

Above all, praise be to ALLAH Almighty, who gave me the ability and patience to overcome all the difficulties that faced me during my doctoral studies.

I express my gratitude to my family, especially my wife, who provided the suitable environment for my studies and which carries some family responsibilities during the study.

All thanks and respect to Assoc.. Prof. Dr. Engin GEDİK. Who accepted me to be a doctoral student and supervised the presentation of this thesis in the best way, and provided me with all scientific and practical support for finishing my studies,

My sincere thanks to the supervising committee, Prof. Dr. Mehmet ÖZKAYMAK and Prof. Dr. Kamil ARSLAN, who provided all the advice and guidance until we got this work to the fullest.

Last however now not least, I would like to thank the team of Energy labs at Karabuk University for their help during the education of experimental setup and testing period.

CONTENTS

Page

Page

Page

LIST OF FIGURES

Page

Page

LIST OF TABLES

Page

SYMBOLS AND ABBREVIATIONS INDEX

LATIN SYMBOLS

A_{th} : Area of the receiver plate [m^2]

I_{sol} : Total incident solar radiation [W/m^2]

m : mass [kg]

P : Electric power [W]

V : Voltage [V]

$\dot{Q}_f$: Useful thermal power [W]

$\dot{Q}_{in}$: Solar radiation incident on the receiver plate [W]

$\dot{Q}_{rad}$: Radiation heat transfer [W]

$\dot{Q}_{conv}$: Convection heat transfer [W]

$\dot{Q}_d$: Heat dissipated by liquid cooled heat sink [W]

ε : Emissivity of the copper receiver plate

K : Thermal conductivity [$W/m^2.K$]

K_f : Thermal conductivity of base fluid [W/m K]

K_n : Thermal conductivity of nanoparticles [W/m K]

$K_{n,f}$: Thermal conductivity of nanofluid [W/m K]

C_p : Specific heat [kJ/kg.k]

$C_{p,n}$: Specific heat of nanoparticles [kJ/kg K]

$C_{p,nf}$: Specific heat of nanofluid [kJ/kg K]

T : Temperature [°C]

$\dot{m}$: Mass flow rate [kg/s]

$\dot{m}_f$: Mass of base fluid [kg]

$\dot{m}_n$: Mass of nanoparticles [kg]

I : Current [A]

σ_e : Electric conductivity

SUBSCRIPTS

n : Nanoparticle

nf : Nanofluid

c : Cold side

h : Hot side

o : Outlet

f : Base fluid

I : Inlet

GREEK SYMBOLS

η_{ele} : Electric efficiency [%]

η_{th} : Thermal efficiency [%]

η_{total} : Total efficiency [%]

$\emptyset$: Volumetric ratio of nanofluid [-]

ρ : Density [kg/m^3]

ρ_f : Density of base fluid [kg/m^3]

ρ_{nf} ; Density of nanofluid [kg/m^3]

ρ_n : Density of nano nanoparticles [kg/m^3]

DIMENSIONLESS GROUPS

Pr : Prandtl number

Nu : Nusselt number

Re : Reynolds number

Ra : Rayleigh number

ZT : Figure-of-merit

CHAPTER 1

INTRODUCTION

1.1. BACKGROUND

If new energy sources aren't added to the present energy reserves, the demand for energy may not be able to keep up with the world's population increase and technological advancements. Currently, the primary energy resources are non-renewable fossil fuels including oil, coal, and natural gas. The combustion of these fossil fuels has had detrimental influence on the environment, including air pollution and global warming. Carbon dioxide CO_2 emission are on the rise, which has raised concerns about change of climate and the sustainability generations of the future over the world.

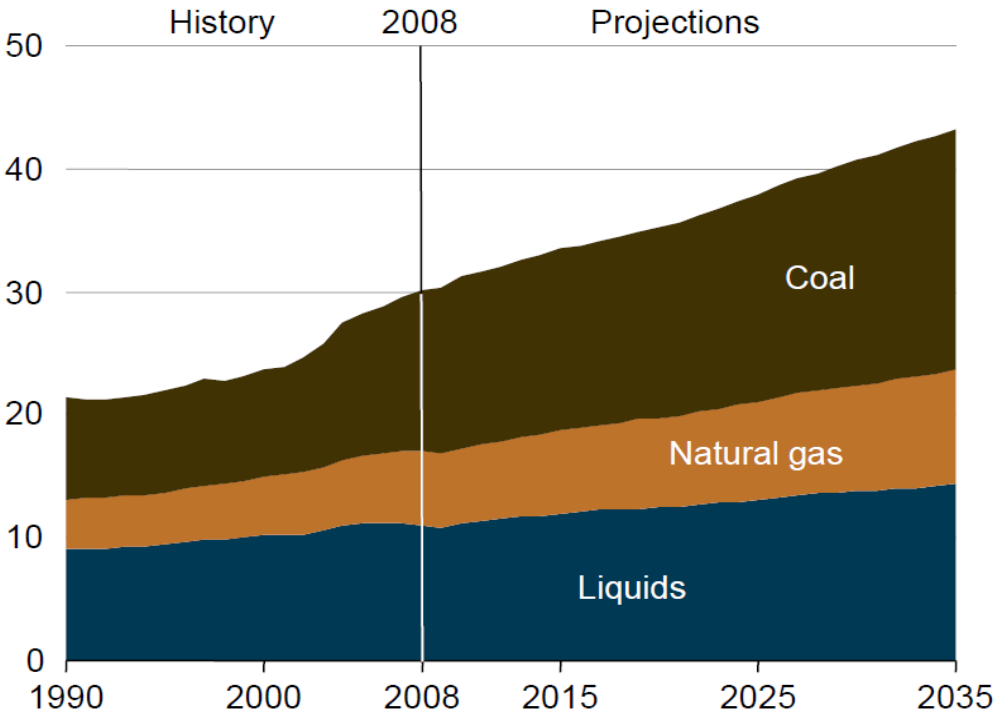

Figure 1.1. Contribution of World energy CO2 emissions.

The rate of CO2 emissions is strongly related to the level of global population, and coal combustion is the essential reason of CO2 emissions among the three fossil fuels depicted in Figure1. According to projections, CO2 emissions would increase in value form 32.2 billion tons metric in 2008to 35.2 billion tons metric in 2020 [1]. Furthermore, by 2035, estimated CO2 emissions are anticipated to increase by 43% to 43.2 billion metric tons. Ideational power plants of coal-fired are anticipated to be put into operation over the next 20 years to produce adequate electricity in order to boost human activities. China, for example, is among the countries with the greatest CO2 emissions due to its rapid economic development and high domestic demand. As a result of this growth, coal consumption is predicted to rise significantly, posing a huge threat to the environment. Between 2008 and 2035, China's coal-fired power plants are anticipated to double in number [1].

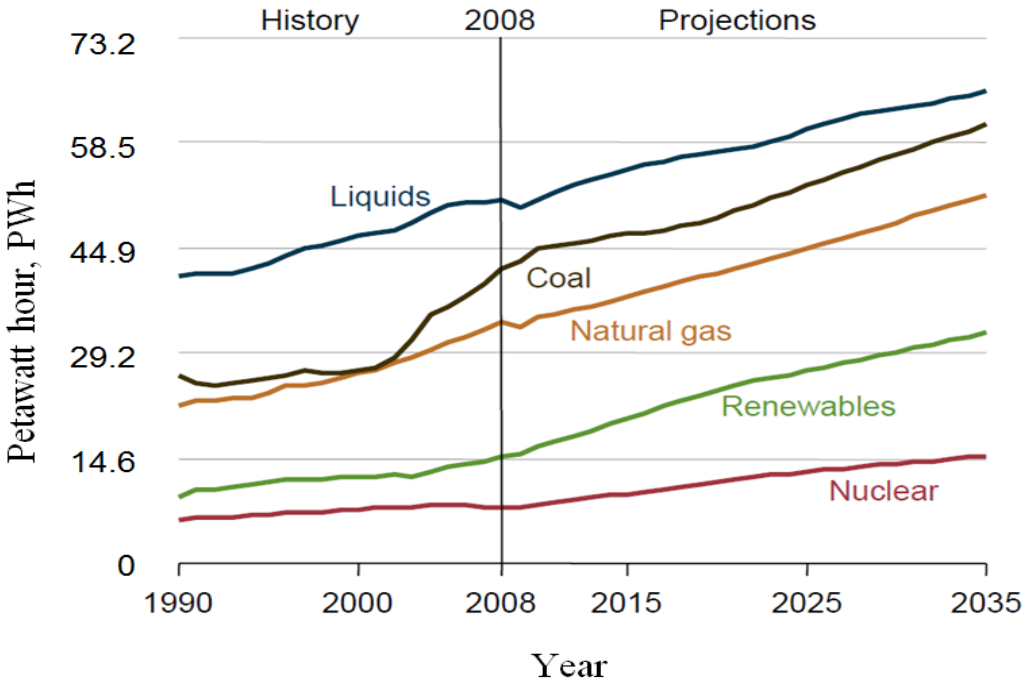

Figure 1.2. World energy consumptions.

In spite of the nuclear energy has a great in potential to meet the world expanding energy demand, concerns about nuclear accidents and incorrect nuclear waste disposal have prevented the construction of nuclear plants. Additionally, the recent tsunami-caused devastation of the Fukushima Daiich nuclear reactors on March 11, 2011, has severely damaged Japan's environment and health[2] . The disaster's

aftermath has also sparked widespread public opposition to and protests against nuclear energy projects and development. These factors will make renewable energy sources a more alluring energy creator in the future.

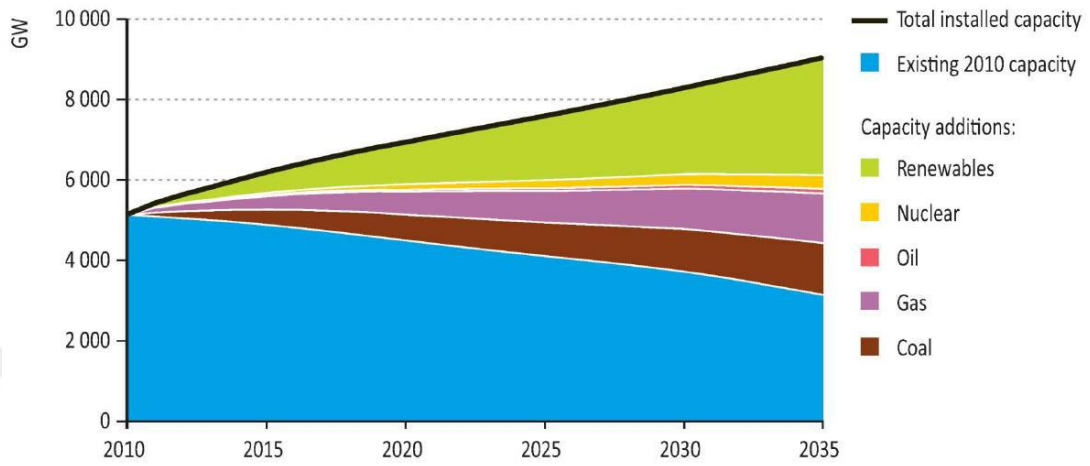

Figure 1.3. Capacity distribution power generation.

Currently, 14% of the world's overall energy request is met by the renewable energy resources [3]. Sources of renewable energy such as thermal, solar, hydropower, geothermal, wind and marine have received a lot of attention recently on a global scale. From figure 1.3, clearly shows that there is potential for rapid expansion in the usage of renewable energy over the next 20 years. Figure 3.1 also, depicts a substantial growth in the predicted renewables of installed capacity through the future decades. By replacing a considerable amount of the dependency on fossil and nuclear fuels, large-scale expansion of renewable sources can reduce the associated environmental impacts. In order to make a extra sustainable and clean society for their future generations, an increasing number of developed nations have started developing in the clean energy technology. The anticipated rapid decline in prices of renewable energy (cost/watt) over the next few years will support this encouraging trend. In order to achieve an inexpensive and sustainable energy future, research into a new renewable energy resources and advancements in current energy harvesting techniques both can play a significant role.

1.2. CONCENTRATING SOLAR ENEGY

On the Earth, solar energy is cheap, clean, and plentiful. On a sunny day, it may produce about 1000W/m^2 of solar energy. Solar power generating cells that may change solar energy into electrical power include photovoltaic (PV) and thermoelectric generating (TEG) cells. Despite the fact that solar energy is free, solar cells utilize an expensive semi-conducting materials and have a low in energy efficiency conversion for example, (conventional poly crystalline based on PVcells have an efficiency of about 17%) [4].

The intensity of solar energy could be enhanced many times depending on the ratio of solar concentration by concentrating the incoming solar radiation using a solar concentrator. Concentration can be used in solar power generation systems to enhance electrical power production or decrease the solar cells number needed to generate a given amount of power. Solar concentration reduces the cost of producing solar electricity by combining fewer, more costly solar cells with a less expensive solar concentrator to produce an equivalent amount of power. For photovoltaic PV concentrated systems and the concentrated thermoelectric generators CTEG, the parabolic trough collectors and Fresnel lens are common forms of solar concentrators.

1.3. PARABOLIC TROUGH COLLECTORS

The collectors of parabolic trough collectors (PTCs) are created by parabolic-shaping a sheet of reflecting subject. Along the line of the focal the receiver plate, b black metal plate is positioned to reduce heat losses (see Figure 1.3). Parallel rays strike the reflector when the parabolic is facing the sun and reflected onto the receiver plate. The fluid that flows through the receiver plate is heated by the focused heat radiation that reaches it, turning solar energy into usable heat. Long collector modules are created since a long collector module is created since a single axis tracking system to track the sun is suitable. The collector can be pointed in east-west, north-south or north-south when tracking the sun from east to west. The complete aperture always faces the sun at the middle of the day, which is a benefit of the previous tracking

mode, but the performance of the collector entire early and lately hours of the day is significantly removed due to a big incident angles cosin losses a single axis tracking of the sun is suitable[5].

1.4. FIELD OF THE RESEARCH

It categorical reviews the transient information and supports the efforts to improve an increasing in electricity production by using solar thermoelectric technology. The outcomes of this study are specified, and can be efficiently joined with sustainable energy sources. It examines and understands the behavior and the capability of the selected solar thermoelectric system to consume less energy.

1.5. RESEARCH METHODS

The main objective of the literature review is to totally know the current problem and the influences on economy and environment of solar thermoelectric technology. It will help to estimate the gaps in efficiency and feasibility in the existing systems and the diverse aspects of CTEGs.

1.5.1. Mathematical Model

This research work includes the development of a mathematical modelling and computer programme. The theoretical mathematical simulation to estimate the performance of the CTEG joined with the thermoelectric cells is additional improved. Experimental results are utilized in order to validate the theoretical model, which can then regulate the optimization also sized system simulation.

1.5.2. Experimental Procedure

In the research work, thermoelectric cells have been utilized for the test the thermal and electrical performances of the concentrated solar power utilizing trough collector. The proposed CTEG system is designed to predict the power production and thermoelectric cells enhancement by utilizing concentrated solar radiations. This

study includes the design detailed, mathematical modelling, as well as, experimental analysis. A mathematical modelling has been validated against the results of the experiment in order to guarantee the validity of the simulation. The model can be utilized as a predict technique for thermal and electrical efficiencies of the concentrated solar power under different design requirements.

1.6. THESIS OBJECTIVES

- To design and constricting a standalone system that could generate electrical power from thermoelectric cells by utilizing a solar thermal energy and to validate the numerical computer model.
- To experimentally investigated influences of multi walled carbon nanotubes distilled water (MWCNT) and graphene nanoplateles distilled water as a coolants on the electrical and thermal efficiencies of CTEGs.
- To develop a mathematical computer model to simulate and anticipate the performance of CTEGs.
- Using a wide range of the solar radiation spectrum.

1.6. STRUCTURE OF THE THESIS

The outcomes of the thesis are described in six chapters. These chapters have the following contents:

Chapter 1: Introduction
Chapter 2: Literature Reviews
Chapter 3: Setup and procedure
Chapter 4: Mathematical model of CTEGs)
Chapter 5: Result and discussion
Chapter 6: Conclusions and Recommendations

CHAPTER 2

LITERATURE REVIEEW

2.1. INTRODUCTION

The necessity for substitutional renewable energy resources like, solar, geothermal and wind energy to reduce the use of fossil fuels is well acknowledged. The combustion of fossil fuels is responsible for the majority of greenhouse emissions. Droughts, hurricanes, and photochemical smog are just a few examples of the phenomena that have been brought on by rising greenhouse gas and air pollution emissions [6]. Solar energy is the abundant, usable, sustainable and large renewable energy source. Both thermal and electrical methods can be used in order to capture this enormous amount of energy. Solar thermoelectric generators are one of the technologies that are utilized in order to change solar energy to electric power and lessen the environmental consequences of greenhouse emissions.

Since the 1950s, research into solar thermoelectric power generation has gained attention. Research on thermoelectric power generation was boosted in the 1960s, and several successful thermoelectric devices were produced [7]. A solid-state process known as thermoelectric production converts temperature gradients directly into electric power and vice versa. Material of thermoelectric element, heat exporter and cooling technique are three crucial factors that can improve TEG efficiency. Similar to a heat engine, a TEG uses charge carriers as the working fluid. It operates quietly, has no moving components, and is quite dependable. Though its use is limited to specialized medical, military, and space applications because to its low efficiency (about 5%). When the heat supply is inexpensive, it has been realized. Many and diverse studied been achieved in the literature about utilizing water to cool TE modules and to reduce their cool surface temperature.

G. MUTHU et al. [8] the behaviour of suggested thermoelectric power production system utilizing a solar parabolic dish collector was theoretically analysed and

experimentally validated. The theoretical analysis and practical findings led to maximum outputs power of 16.43 W and 15.35 W, respectively. Between theoretical and experimental results, there is an average error of 11.12% and a standard deviation of 0.869, respectively. The uncertainty of the electrical power of the system is 2.07%.

S. Shanmugam et al. [9] conducted modelling and experimental validation of a thermoelectric power production. The model consists of the dish collector with the diameter of 3.56 m, focal length of 1.11 m, height of 70 cm and a flat receiver was built of a 30cm square aluminium slab with 3mm thickness and four thermoelectric cells and the manual tracking system. The study outcomes reveal that the system was capable of producing electric power point of 14.7 W, moreover, the result of the modelling were compared with experimental outcomes and there were in 10% accuracy.

Fan et al. [10] manufactured and experimentally tested a concentrated solar thermoelectric system utilizing parabolic dish collector. The experimental results of the system showed that the model was capable to generate electric power up to 5.9 W at the temperature variation of 35°C and the temperature of the hot side 68 °C.

In the nanofluids application for the thermal performance growing of thermoelectric systems, many research studies were achieved. Li et. al [11]utilized a graphene distilled water as a heat transfer coolant in the mini channel to increase the efficiency of TEG and tested the performance of the generator thermoelectric cells at lower temperatures. When the selected nanofluid was compared to the distilled water the better of the voltage, output power and conversion efficiency were achieved whereas the increment in the outcomes were 11.29%and 3.5% respectively.

Ahammed et. al [12] inspected the feasibility of utilizing nanofluid in thermoelectric cooling of an electronic device. Base on Al_2O_3/distilled water nanofluid with the volume concentrations divers between 0.1%and 0.2% was applied as working fluid stream in a small channel heat exchanger to take of the heat from the TE cold side temperature. An improve of 9.15% in the temperature

difference between the hot and cold sides of thermoelectric was achieve utilizing (0.2 vol%) nanofluids, as a result, the capacity module of the cooling was improved.

Zhou et Al. [13] analysed the efficiency of the TEG using water based CuO nanofluid. As a compared to water, it was notice that the output power from a small size of TEG increased 38%.

Karana et al. [14] utilized EG-W, ZnO and MgO based nanofluid for the thermoelectric system. They were examined the influences of different parameters like inlet temperature, Reynolds number, device total area, type of nanofluid and concentration of nanofluid particles on the output power, conversion efficiency and generated voltage of TEG. It was found that the nanofluid of MgO nanoparticles increased the voltage of the TEG.

Li et al. [15] the performance of thermoelectric based on automotive using waste heat recovery system was compared by utilizing (ethylene glycol) Cu-EG nanofluid and EG-distilled water. It was observed that the used of Cu-EG nanofluid , the power achieved and conversion efficiency was higher than when utilizing EG-distilled water. Moreover, for volume fraction of 0.3 nanofluid the evaluated output power 13.90% increased.

Nnanna etal. [16] conducted a theoretical study by utilizing nanofluid based heat exchanger in order to cool a thermoelectric generator putted between a heat exchanger and an integrated chip Al_2O_3/H_2O nanofluid utilized with 27 nm particle size and volume fraction variable between 1% and 2%. The selected nanofluid improved the thermal contact resistance between heat resource and TE device, which in turn improve the total efficiency.

Mohammadian et al. [17] studied the influence of utilizing Al_2O_3- pure water nanofluid in micro fin heat exchanger on the the thermoelectric generator performance. The results showed that by utilizing low volume fraction with low value of nanoparticles in the heat exchanger which leads to enhance in magnitude the coefficient of the system performance of the TE module at the lower Reynolds

numbers, while utilizing nonparticels in the heat exchanger cold surface led to increase in performance coefficient at higher Reynolda number.

Abdelkareem et al. [18] presented the outlooks of thermoelectric generators with nanofluids. The review included the specialized uses of TEG systems because of their significant contribution to cost reduction and the resolution of numerous environmental problems associated with the usage of fossil fuels. Additionally, they showed that TEG applications are a promising waste heat recovery (WHR) device that can be used for direct heat to power conversion, particularly if these systems were linked to heat transfer improvement technology like nanotechnology.

Tahsin et al. [19] investigated the influences of heat pipes fill of nanoparticles (MgO) and water and on electrical production. Some thermal and electrical quantities such as Seebeck coefficient, maximum output power, thermal resistance and electrical efficiency were estimated by using the collected experimental data. The experimental outcomes showed up that water is adequate for utilizing as working fluid according to climax geography of the implemented model. this means that there is not necessary to use nano-particles as working fluid in this study.

Chang et al. [20] inspected the utilize of a solar thermoelectric device for generating electricity from the solar energy. They utilized electrophoresis deposition manner to construct CuO soft film by depositing self-prepared CuO nanofluid onto the Cu plate, which involve between sensitized solar cells and TE module. It was found that the system produced about 4.90mW/cm^2 when 100 mW/cm^2 intensity of solar irradiance was utilized. Also, the utilize of CuO soft film coating on its surface increased the temperature approximately 2°C and the voltage about 14.8% and to sum up, the conversion efficiency was increased approximately 10%.

Ahmmed et al. [21] they used graphene/water nanofluid to increase system performance in mini channel heat exchanger jointed with thermoelectric generator. The results showed that the system performance of TE module increased at about 72% when the graphene nanofluid distilled water was utilized. Moreover, convective HTC was improved by 88.62%.

P. Sundarraj et al. [22] carried out a modelling and experimental analysis of the thermal and electrical performance of a hybrid system(HSTEG) of solar thermoelectric generator. The experimental result showed that the system HSTEG is able of generating a high electrical output power of 4.7W, the 1.2% electrical efficiency and 62% thermal efficiency for the 92 °C mean temperature difference against the TEG generator with 382 W input heater power. The outcomes showed that the experimental of the system are found to be in good acceptance with the theoretical evaluation.

Sravan Kasireddy et al. [23] used a novel method in order to change the solar energy into electrical power by utilizing a thermoelectric generators and parabolic trough collector. Three thermocouple substances which were iron, copper and constantan were utilized for every of three reflecting surfaces glass, stainless steel and acrylic to achieve the experiments. The outcomes showed that the system was able of producing conversion efficiency of o.o1%, voltage 38 mV, current 0.01A and 59°C temperature difference when iron constantan thermocouple were used.

C. Lertsatitthanakorn et al. [24] constructed a new model for producing electrical power generation consists of a 1.5 meter parabolic dish collector with an aperture area of 10 × 10 cm^2 receiver plate. One BiTe based thermoelectric generator mounted on the copper receiver plate. A fin heat sink of a rectangular shape fan coupled with was utilized to remove the heat from the cold side of thermoelectric module and a mechanical tracking system was utilized to track the sun continuously. The outcomes revels that, the thermoelectric module was capable of producing 1.32 W at air flow rate of 0.42 m^3/min pushing air according to 2.89% conversion efficiency.

Kewen et al. [25] conducted a laboratory experiments to calculate the output power at several distilled water flow rates, many temperature difference between the hot and cold sides were achieved. The five thermoelectric cells were capable to generate about 4.7 W electric power with a 72.2°C temperature difference between hot and cold sides. The achieved output power from each module was about 0.5W at these temperature variations. The data of the experimental can be utilized to the design

Commercial TEG generators.

Rehman et al. [26] conducted a simulation work showed that some affected parameters on the surface of thermoelectric cells and the optical efficiency. For the receiver configuration the highest optical efficiency of 93.61% was estimated. Moreover, the electrical efficiency of 1.45% was achieved at 50.8 °C difference in temperature.

Yang et al. [27] suggested a numerical model to estimate the performance of thermoelectric module with optical concentration. The results of the study showed that the electric efficiency of the model decreased to 3.85% and had 61.5% relative drop when the overall heat losses and contact resistance were taken into account.

L. Miao et al. [28] constructed a prototype of solar thermoelectric generator (STEG) consists of a selective absorber SSA film, six thermoelectric cells, a compressed water flow rate and a concentrator parabolic trough collector with aperture area of $2*2m^2$. The results of the experiment showed up the electrical conversion efficiency, and total efficiency of the system under the best conditions of environmental and insolation of solar were 1.14% and 49.5% respectively. Finally, the overall system was capable to produce electrical power of 18W; moreover, 2 L/min of hot water at 37 C was achieved and stored in the insulated tank.

R. Bjork et al. [29] tested the performance of combined solar thermoelectric generator and solar photovoltaic utilizing theoretical model for several kinds of commercial PVand bismuth telluried TEG. In order to achieve the same temperature the thermoelectric is applied on the back of the PVcell. The results of the this theoretical survey showed up that for the cases of crystalline Si and selenide (CIGS). The combined PV cells system generated a lower output power and lower efficiency than PV alone. As a result of this study a joined thermoelectric and photovoltaic for power production was not viable choice.

Edgar Arturo et al. [30] performed an experimental study of a concentrating solar system based upon thermoelectric generators (TEGs). Their system include 6 TEGs

connected serially for electrical generating with based upon a traditional Bi_2Te_3semiconductor material, which was illuminated by concentrated solar irradiance on one side and cooled by flowing pure water on the other side. The results of the system showed that, 20W of electric power could be achieved and 200 W of thermal energy stored in water tank. The 5% electrical efficiency and 50% thermal efficiency can be achieved with the evaluated the price of electrical power production which are approximately near from photovoltaic and thermal systems

Chao Li et al. [31] examined the influences some parameters environmental on the conversion efficiency for the new standalone power supply utilizing parabolic trough collector coupled with thermoelectric modules. The outcomes of this study show up that the environmental conditions such as solar insolation, ambient temperature and wind speed are strongly affected on system performance. By increasing some parameters like the solar radiation, ambient temperature and wind speed the thermal losses of the system increased. While, the increased in solar insolation leads to electrical efficiency enhancement, moreover, the increased in wind speed and ambient temperature causes in electrical efficiency decreased.

Omer et al. [32] conducted a system design and simulation study of two stage concentrator thermoelectric generator for generation electric power. A second stage trough collector was utilised. A secondary parabolic collector positioned at the focal point of the trough collector. TEG commercially available was utilized in the solar receiver tube. For removing waste heat and maintain a higher heat gradient across the TE the cooling tube was used. The simulation result was conducted by utilizing computational fluid dynamic modelling. The outcomes showed up that misalignment as much as 4 degree could decrease in thermal efficiency.

The main objective in this study is to utilize the carbon nanomaterials for increasing the CTEGs performance. The graphene nanoplatelets and MWCNT nanofluids were experimentally investigated for the first time to date in this study, to cool a concentrator thermoelectric generator (CTEG) module and to increase its performance. The pure water was also utized in this study to achieve this objective, the CTEGs module was fabricated and the experimental setup was decided in

Karabuk University, Turkey. The constructed CTEG system was outdoor examined under the Turkish climate conditions of 0.25 wt% and 0.5 wt% nanofluids concentration and pure water, at 0.5 L/m coolants flow rate. The experimental outcomes of the system with nanofluid coolants were analysed from energetic viewpoint.

CHAPTER 3

SETUP AND PROCEDURE

3.1. EXPERIMENTAL SETUP

The system setup was designed and fabricated in labs of Karabük University in Türkiye. Between the receiver plate and cooling duct, the experimental setup includes five thermoelectric modules (model No: TEG1-24111-6.0) attached in a set. Also, it has a trough collector adjusted manually to track the sun facing to the south direction continuously. The picture and graphical illustration of experimental system were given in Figures 3.1 and 3.2.

Figure 3.1. Setup view with piping system and storage tanks.

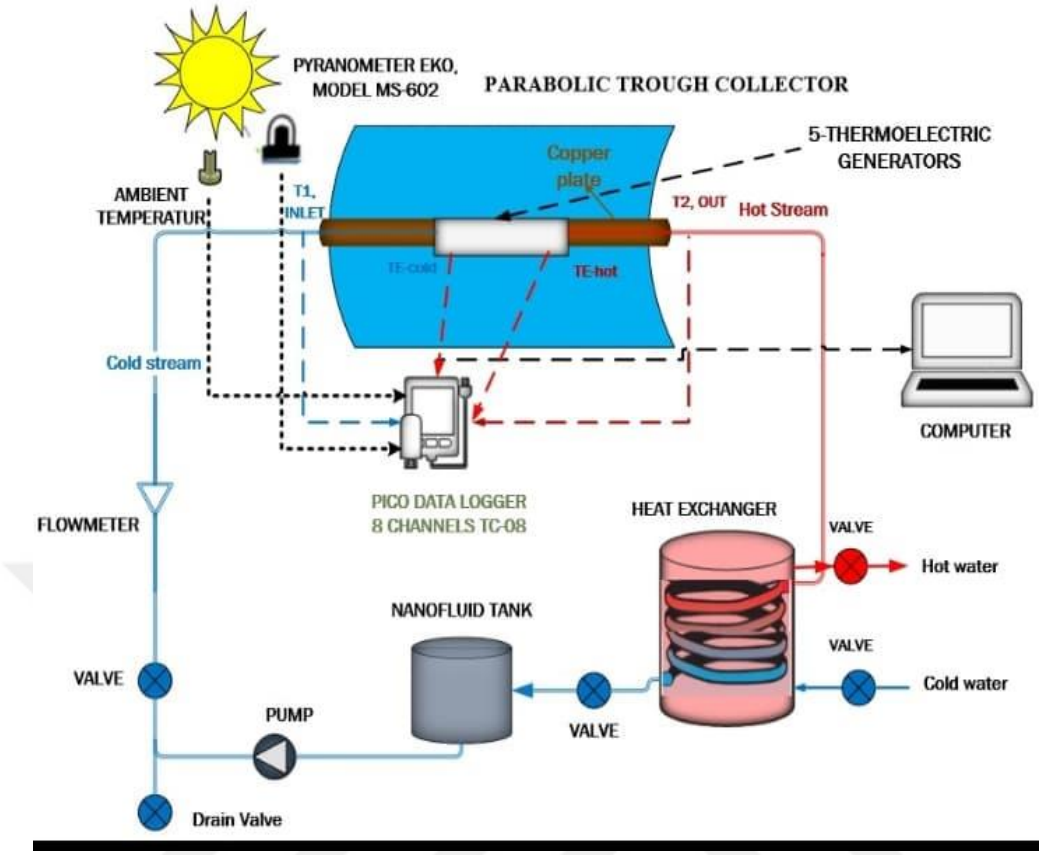

Figure 3.2. Graphical illustration of experimental system.

To ensure a perfect connect a thermal conductive paste (k_{paste}=3 W/m°C) was dispersal between the back surface of the receiver plate and thermoelectric generators. As shown in the previous figures, the system contains a heat exchanger, nanofluid storage tank then a variable speed pump was used to circulate coolants throughout system ducts and also the nanofluid's volumetric rate measured flow meter was attached. For temperatures measurement, data logger connected by K type thermocouples with systems parts to measure inlet and outlet temperatures of fluid in cooling duct, surface temperatures of thermoelectric cells and ambient temperature. A Pyranometer device was used for overall solar radiation. Constant resistor loads were connected to thermoelectric generators (TEGs) to achieve the maximum electrical output power and guarantee a continued production of electricity from thermoelectric generators. Constant resistor loads were connected to thermoelectric generators (TEGs) to obtain the maximum output power of electricity and to ensure a continual generation. Furthermore, all parameters were measured every 20 s and imported to laptop simultaneously.

3.2. PARTS AND INGREDIENTS OF THE EXPERIMENTAL SETUP

3.2.1. The Trough Collector

The trough collector is manufactured by curvaturing a sheet of reflective material into a parabolic trough shape as shown in figure 3.3.

Figure 3.3. Image for the trough collector.

The receiver plate of the trough collector is linear along the focal line. The parameters design of the solar trough collector are given in table 3.1.

Table 3.1. Design specification of trough collector

CTEG Specifications	Measures
Collector length	0.9 m
Aperture width	0.6 m
Aperture area	0.54 m^2
Tracking mechanism	Mechanical
Support structure material	mild steel
Focal distance	0.26 m

3.3.2. Receiver Unit

The receiver plate is made from a copper plate subjected to aperture area of the trough collector in order to absorb the concentrated solar radiation to supply the heat to thermoelectric generator. The volume of heat absorbed by the receiver plate is depending mainly on reflective material. The receiver plate is 10mm thick and has an area of 0.054 m^2.

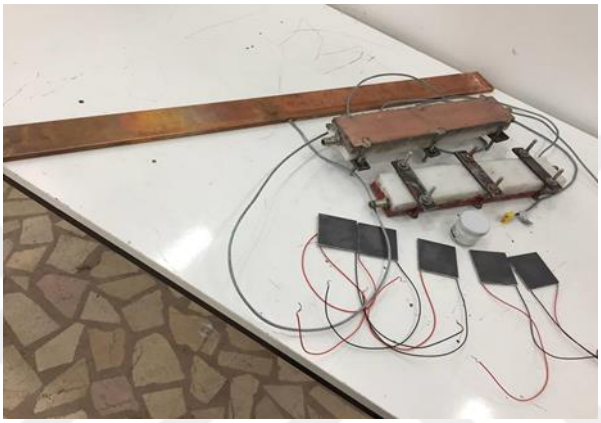

Figure 3.4. A diagram of heat transfer system.

In order to create a low temperature of the cold side of thermoelectric generator the coolant will be utilized for heat removing. For the used material of the cooling system, the lower section is made from the copper plate whereas the upper part is made from polyethylene material. The dimensions of the internal cooling duct is 6cm*34cm*2.5cm. At the middle of the cooling system the thermocouples were fixative in order to measure the temperature of copper plate, which assumed to be the same temperature as the cold side thermoelectric temperature.

3.2.2. Thermoelectric Generators

Thermoelectric cells utilize semiconductor material of n-type and p-type Bismuth Telluride. Bismuth Telluride is a semi-conducting material which has captivating electrical properties of high Seebeck coefficient (~190μV/K) and high figure of merit (~2x10-3 1/K). In the proposed system, five series- thermoelectric modules (TEG 1-

24111-6.0) with single dimensions of 56*56 mm^2 and 127 p-n junctions in each module are used. The specifications of TEGs are illustrated in Table 3.2.

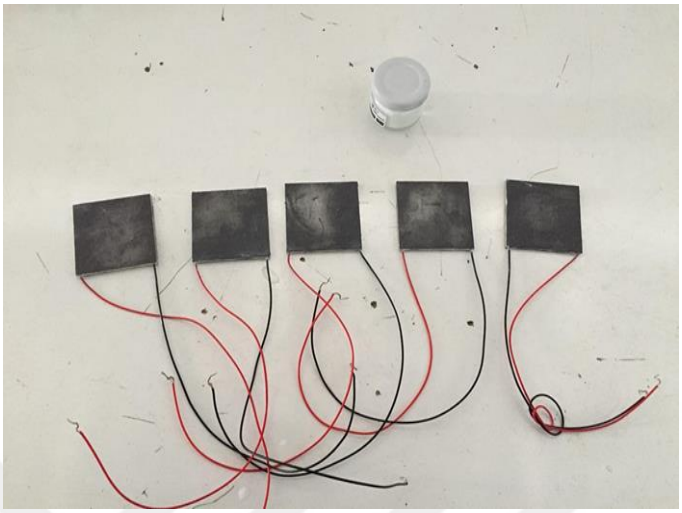

Figure 3.5. Image of used TE cells.

Table 3.2. Specification of used thermoelectric cells.

TEG specifications	Measures
Hot side temperature	300
Cold side temperature	30
Matched load resistance (ohms)	4.4
Open circuit voltage V	17.7
Matched load current A	2
Matched load voltage V	8.8
Matched load power W	17.6
Number of thermocouples	127
Number of modules	5

3.2.3. Storage Tank

According to the size evaluation of the storage tank the area of the collector can be estimated as the following.

The area of the collector = 0.60*0.90 = 0.54 m^2

With the proposed overall area in this setup of 0.54 m^2 for collector, 40 L storage tank was designed and manufactured. The coil of heat exchanger is made from the copper metal while the storage tank is made from stainless steel sheet.

Figure 3.6. Manufactured of storage tank.

3.2.4. Nanofluid Tank

The nanofluid tank is fabricated with size of approximately 6 L. It facilitates the filling and draining procedures of working fluids with small losses of fluids quantity.

Figure 3.7. Image of Manufactured Nanofluid tank.

3.2.5. The Circulation Pump

In order to circulate the working fluid into the components of the experimental setup, a circulating pump with a variable speed from Nova company, model: RS25/4G-130 was utilized. The pump acts at three speed levels and works under the fluid temperature terms from -10 °C to 110 °C.

3.2.6. Air Vent

The air vent was putted at the top point in the experimental setup in order to release the air from the working fluid.

Figure 3.8. Air vent image.

3.3. RUNNING THE EXPERIMENTAL SETUP

After finishing the assembly of experimental setup, calibration has been done for temperature, flow rate, voltage, current and solar radiation

The calibration of the flow rate was done by using a container of 1000 mL volume and stopwatch.

The calibration of the solar radiation was conducted by utilizing two types CEM DT-1307 solar meters during the working range of the experimental.

The calibration of voltages and currents were done by using different two types of clamp multimeter of model UNI-T UT203.

In order to run the experimental setup, in every experiment the following processes were conducted:

- Shift the experimental model to south direction face.

- Fill the storage tank of the nanofluid approximately 3 litters of the coolants, the pipe line in that way from the coolant storage tank to the circulation pump should be totally full in the coolant.
- Operate the circulation pump after that, open the air vent in order to remove the air from pipeline of the system, which may create flow blockage, after that, when the uniform stream of working fluid is noted without any air bubbles shut down the air vent.
- Setting the control valve in order to monitor the desirable flow rate of the active fluid.
- After the storage tank is filled by the city water, setting the control valve in order to control the rate of flow city water flow.
- Before start logging, running the system for 5 min in order to get thermal equilibrium situation.
- Starting the logging operations for temperatures with Pico USB TC-08 data logger every 20 seconds and for voltage, current and solar radiation at every 5 min.

For cleaning the pipeline and changing the working fluid:

- Operate the circulation pump.
- Open the outlet valve in nanofluid storage tank to get away the main fluid from the system pipe line with keeping the pump on.
- After the main fluid getting out from the nanofluid storage tank and no more fluid passing into the nanofluid tank, shut down the pump and then close the drain valve, from the pump exit remove the rubber pipeline and the air vent should be completely open. In order to remove the residue of working fluid by giving an air blow from the pipe line tube to push out from the cooling duct and pipeline to the nanofluid storage tank and to the out of the pipeline from the exit side pump. Let the main fluid get out by opening the drain valve
- In order to clean the system, join the pipeline into the circulation pump and fill the nanofluid storage tank with clean city water as mentioned above. To let the unclean fluid out open the drain valve and turn on the pump. By Keeping the pump on and the drain valve open, by observing the changing

colour of the working fluid. Turn off the pump when all of the working fluid is changing to the clear city water, drain the fluid and clean the piping system.

3.4. NANOFLUIDS USED IN THIS STUDY

A single film graphene nanoplatelets aquatic dispersal (thickness of 0.55-1.2 nm, diameter of 1-12μm, specific surface area of 500-1200 m^2/g and purity more than 99.3wt%) and for MWCNTs –water dispersal (outside diameter of 18-28 nm, length of 8-35 μm and purity more than 96%) were taken from NANOGRAFI Co. Ltd. The concentrations 0.25% and 0.50% nanofluids were provided. Table 3.4 presented the thermophysical properties of nanoparticles and water. These properties of MWCNT nanoparticles water [33], graphene nanoplatelets water [34] and water [35] were taken from the literature.

The images of graphene nanoplatelets and for MWCNTs are shown in Figure 3.4. During the experiments period no sedimentation was observed.

Figure 3.9. Samples of nanofluids used in the experiments.

Table 3.2. Thermo-physical Properties of nanoparticles and pure water.

Material	ρ, **(kg/m^3)**	**K, (W/m K)**	C_p, **(kJ/kg K)**
MWCNT-Water	1600	3000	0.796
Graphene-Water	2100	5000	0.710
Distilled water	997	0.607	4.180

3.4. PARAMETERS CALCULATION OF NANOFLUIDS THERMAL PROPERTIES

The prepared thermal features of nanofluids can be estimated from the main fluid and the nanoparticles properties at the bulk temperature [36].

The density of nanofluid can be calculated by using Pak and Cho model [37].

$$\rho_{nf} = \emptyset.\rho_n + (1-\emptyset).\rho_f \quad (3.1)$$

Xuan and Roetzel model [38] can be used for calculating the heat capacity of nanofluid as the following.

$$(\rho_{nf}.C_{p,nf}) = \emptyset.(\rho_n.C_{p,n}) + (1-\emptyset).(\rho_f.C_{p,f}) \quad (3.2)$$

For thermal conductivity Maxwell-Garnet model [39] as follows

$$K_{nf} = K_f \frac{K_n+2K_f-2\emptyset(K_f-K_n)}{K_n+2K_f+\emptyset(K_f-K_n)} \quad (3.3)$$

Where: ρ is the density (kg/m^3), C_p is the specific heat($kJ/Kg\ K$), K is the thermal conductivity ($W/m\ K$) and $\emptyset$ is the base fluid volumetric ratio of nanoparticles in a suspension solution. The subscripts n, f, and nf stand for nano-particles, base fluid and nanofluid respectively.

The volumetric ratio$\emptyset$ of the nanoparticles in the solution of the base fluid can be evaluated by the following relation.

$$\emptyset = \frac{m_n/\rho_n}{m_n/\rho_n+m_f/\rho_f} \quad (3.4)$$

Where $m_f\ and\ m_n$ are the mass of the base fluid and nanoparticles respectively.

The useful thermal power Q_u (W) in the system gained by the coolant is given by:

$$Q_u = \dot{m} \times C_p(T_o - T_i) \tag{3.5}$$

Where $\dot{m}$, C_p, T_i and T_o are mass flow rate of the coolant (kg/s), specific heat of the coolant $J/(kg.K)$, inlet fluid temperature and outlet fluid temperature respectively.

The generated electrical power P (W) from the thermoelectric cells is given by:

$$P = I \times V \tag{3.6}$$

Where I is the current (A), and V is the voltage (V).

The total efficiency of CTEG system represents the energy amount (thermal and electrical) that TEG can be extracted from the solar irradiance. The thermal (η_{Th}) and electrical (η_{ele}) efficiencies can be calculated as:

$$\eta_{Th} = \frac{Q_u}{I_{sol} \times A_{th}} \tag{3.7}$$

$$\eta_{ele} = \frac{P}{I_{sol} \times A_{TE}} \tag{3.8}$$

Where, I_{sol} and A_{th} are the overall incident solar irradiance on the receiver pate, area of the receiver plate m^2.

The overall efficiency of system which can be estimated as:

$$\eta_{tot} = \eta_{th} + \eta_{ele} \tag{3.9}$$

CHAPTER 4

SYSTEM ANALYSIS AND MATHEMATICAL MODELING

4.1. INTRODUTION

This chapter includes a detailed characterization and system analysis of combine thermoelectric idea solar power concentred systems. The concentrated thermoelectric generator is chosen to be as a solar electric based on CSP system for electrical power production. The main reason of this work is to design and to create a novel model for power generation utilizing thermoelectric cells.

The CTEG system is broken down to two separated sections: theoretical modelling analysis and experimental evaluation. Chapter 4 the current chapter is including the system analyses framework and model description. A mathematical modelling is conducted for evaluating some parameters such as voltage, current, power output, thermal efficiency and electrical efficiency of the proposed system under different parametric terms. The next chapter (chapter 5) includes an experimental evaluation and assessment over the actual test rig.

4.2. DESCRIPTION OF CTEG SYSTEM

The CTEG consists of two ingredients. The first part is the collector, which encloses the solar radiation in the shape of thermal energy. The second part is a thermoelectric cells, which utilizes the besieged thermal energy into its hot joint in order to create current. The thermoelectric equipment’s design has been incorporated, but solar collectors configurations change widely.

The solar radiation concentrated by the trough concentrator supplies the heat resource for the hot side of the TEG generators which can be combined near the focal

length of the trough collector, the other face of the thermoelectric cell is cooled by coolants in order to create a big temperature difference against the cells. As a result, according to the Seebeck influence, the temperature difference is proportional to the potential difference against the two sides of the TE cells, which means, when jointed to the external load, electric power could be generated.

4.3. ENERGY BALANCE FOR CTEG SYSTEM

In proposed CTEG system, the solar irradiance inverted from the trough reflector is absorbed by the copper receiver plate after that passed inside the thermoelectric generator (TEG). A section from this thermal energy is changed into electrical power and the rest of the thermal energy is transferred as waste heat by coolants. The overall thermal loss to the surroundings from the receiver plate is due to natural convection and radiation losses. Thus, the equation of energy balance for the TEG system can be calculated as.

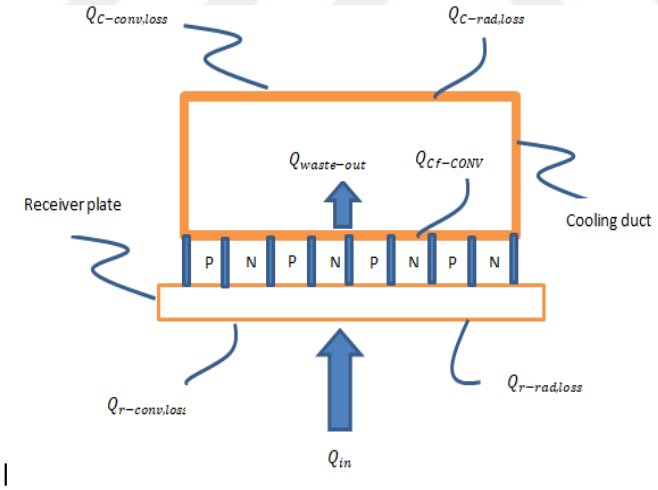

Figure 4.1. Energy balance for thermoelectric cells.

$$\dot{Q}_{in} = P_{TEG} + \dot{Q}_d + \dot{Q}_{rad} + \dot{Q}_{conv} \quad (4.1)$$

The overall energy input per time unit of the CTEG includes convection heat losses $\dot{Q}_{conv}$, radiation heat transfer $\dot{Q}_{rad}$, power generation of thermelectric P_{TEG} and the heat dissipated by coolant $\dot{Q}_d$. The volume of the concentrated solar power

utilized to the heat collector is controlled by the specific ratio of solar concentration, the heating power could be written as:

$$Q_{in} = \eta_{optical} \times I_{sol} \times CR \times A_r \quad (4.2)$$

The arriving solar irradiance is the amount of energy input on the area of the collector of 90cm length and 6cm width. The heat collector illuminated area is similar sized to the overall area of five TEGs (50mm x 50mm). The dimensions of the collector solar concentrator are 900mm (length) by 600mm (width). The concentration ratio of the solar is the ratio of aperture area of the collector concentrator (trough collector) to the heat collector area (receiver plate).

$$CR = \frac{A_T}{A_r} \quad (4.3)$$

The optical efficiencies of these systems are typically within the range of 73%–81% in this modelling assuming of 800–1000 W /m^2 of direct solar irradiance [7].

The energy losses by convection $\dot{Q}_{conv}$ and radiation $\dot{Q}_{rad}$ heat transfer will be input in the total energy absorbed into the system.

$$\dot{Q}_{Conv} = h_{air} A_r (T_r - T_{amb}) + h_{air} A_w (T_{C-ave} - T_{amb}) \quad (4.4)$$

$$\dot{Q}_{rad} = \sigma \varepsilon_r A_r (T_r^4 - T_{amb}^4) + \sigma \varepsilon_c A_w (T_{C-ave}^4 - T_{amb}^4) \quad (4.5)$$

Where A_r is the receiver plate area and A_w is the total cooling area.

The assumption made for losses heat into the surrounding is trough radiation and convection heat transfer with ambient conditions of 1 m/s wind speed was used in the simulation results. The Stefan-Boltzman constant is used to radiation heat transfer, while the coefficient of convective heat for receiver plate can be estimated by [40].

$$h_{air} = 5.7 + 3.8\, V_{air} \quad (4.6)$$

Where V_{air} is the wind speed (m/s).

In order to estimate the heat transfer coefficient at both side of the boundary layers of cooling duct the average bulk temperature of feeding part $\frac{T_{in}+T_{out}}{2}$ should be utilized. Graetz –Leveque.

$$N_u = \frac{hL}{k} = 1.86(R_e P_r \frac{d_h}{L})^{0.33},\ d_h = \frac{4A_c}{P_e} \quad (4.7)$$

This relation can be utilized for laminar flow ($R_e < 2100$). In contrast, the next relation can be used for turbulent flow (2500 < Re < 105 and 0.6 < Pr < 1).

$$N_u = \frac{hL}{k} = 0.023 {R_e}^{0.8} {P_r}^{n} \quad (4.8)$$

Where n is equal to 0.3 for cooling and 0.4 for heating.

The physical data available of coolants can be utilized to calculate some dimensionless group such as Reynold numbe , Nusselt number and Prandtl number.

4.4. TEG ELECTRICAL POWER AND THERMAL RESISTANCE

In this model the commercial available TEGs are Bismuth Telluride (Bi_2Te_3) which are widely utilized of dimensions 50mm (length)* 50mm (width). The temperature difference ΔT_{teg} between hot side T_h and cold side T_c of the module calculate the amount of the output power P_{teg} . the output power could be calculated by[7].

$$P_{teg} = F.N.\Delta T_{teg}^2 \left(\frac{S^2}{2\rho_{teg}}\right)\left(\frac{A_L}{L}\right) \quad (4.9)$$

$$V_{oc} = 2NS\Delta T_{teg} \quad (4.10)$$

Where

$$\Delta T_{teg} = T_h - T_c \tag{4.11}$$

The generated thermoelectric power is controlled by the electrical characteristics where A_L is the thermo-element area, L is the thermo-element leg length of, S is the Seebeck coefficient, ρ_{teg} is the electrical resistivity, N is the thermocouples numbers and F is the quality factor of the manufacture.

Figure 4.2 explains the schematic shape of the CTEG power unit which consists of the receiver plate as the heat source and the cooling duct based heat spreader as waste heat dissipation. The heat collector and spreader are made of copper material due to a high thermal conductivity kcu=401W/m.k^{-1}. The hot side and cold side of thermoelectric are putted between the copper blocks in order to supply temperature difference for thermoelectric power production.

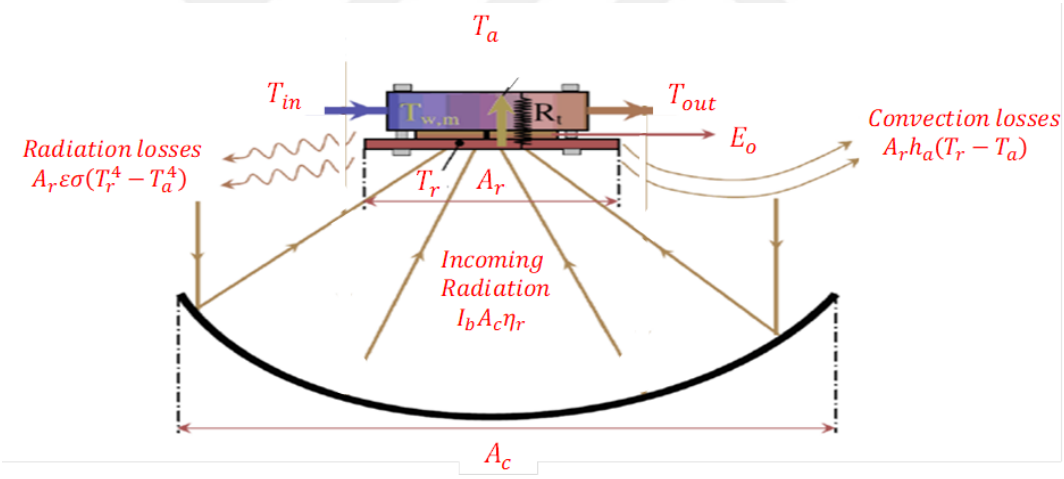

Figure 4.2. Energy flow in the CTEG system.

Figure 4.3 represents the thermal resistance grid from the heat collector to the upper surface of cooling duct. For single TEG the thermal resistance of 1.14CW^{-1} is estimated during the experimental trial [41] . The copper heat collector area and heat spreader area have the same in contact area as five placed TEGs, thermal resistances are calculated as;

$$R_{1-2} = \frac{t_{co}}{K_{co} A_{co}} \tag{4.12}$$

$$R_{3-4} = \frac{t_{co}}{K_{co}A_{co}} \tag{4.13}$$

$$R_{4-5} = \frac{1}{h_c A_c} \tag{4.14}$$

The TEG thermal resistance can be estimated by the following equation

$$R_{2-3} = \frac{t_{teg}}{K_{teg}A_{teg}} \tag{4.15}$$

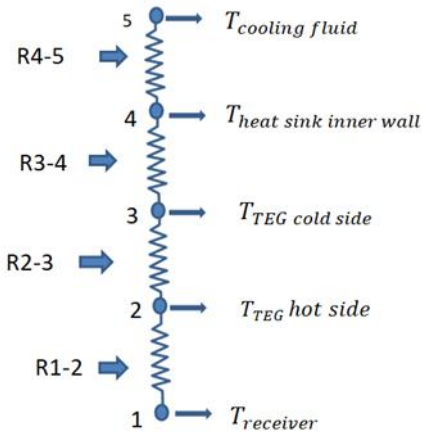

Figure 4.3. Diagram of thermal resistance.

4.5. CALCULATION OF STEADY STATE TEMPERATURE

The specifics of the energy stream via the concentrator thermoelectric generator model are depicted in Figure 3.10. The overall thermal resistance for the heat stream from the incident solar radiation of the receiver plate face to the coolant passing throughout the liquid cooled heat sink determines how much waste heat is wasted by the cooling duct from the cold side of the thermoelectric generators.

Heat removed by a liquid cooled heat sink for the CTEG system can be expressed as

$$\dot{Q}_d = \frac{T_r - T_{cf}}{R_t} \tag{4.16}$$

Here, R_t is the total thermal resistance and T_{cf} is the mean cooling fluid temperature can be determined as $\frac{T_{in}+T_{out}}{2}$

The value of thermal energy output$\dot{Q}_f$ is the useful achieved power (W) by the working fluid in terms of temperature difference can be described as the following:

$$\dot{Q}_f = \dot{m}c_p\left(T_{f,out} - T_{f,in}\right) \tag{4.17}$$

The steady state temperature can be estimated by rearranging equation (4.1) gives

$$\dot{Q}_{in} - \dot{Q}_{rad} - \dot{Q}_{conv} = \dot{Q}_d + P_{TEG} \tag{4.18}$$

Where the term $(\dot{Q}_{in} - \dot{Q}_{rad} - \dot{Q}_{conv})$ the left-hand side explains the real heat passing into the hot side of the TEG module. The generated electric power by the thermoelectric generator can be explained in case of the generator efficiency as

$$P_{TEG} = \eta_{TEG}(\dot{Q}_{in} - \dot{Q}_l) \tag{4.19}$$

Where

$$\dot{Q}_l = \dot{Q}_{rad} + \dot{Q}_{conv} \tag{4.20}$$

Substituting P_{teg} from equation (4.18) and rearranging terms in equation (4.18) gives

$$\left(\dot{Q}_{in} - \dot{Q}_{rad} - \dot{Q}_{conv}\right)(1 - \eta_{TEG}) = \dot{Q}_d \tag{4.21}$$

Where η_{TEG} is the efficiency of the TEG module can be determined from the following equation[10]

$$\eta_{TEG} = \frac{T_H - T_C(\sqrt{1+(ZT)_M} - 1)}{T_H(\sqrt{1+(ZT)_M} + \frac{T_C}{T_H})} \tag{4.22}$$

The dimensionless figure of merit $(ZT)_M$ of TEG is defined as [22]

$$ZT_M = (S^2\sigma_e/k) * T \quad (4.23)$$

Where S is the Seebeck coefficient, σ_e is the electric conductivity, k is the thermal conductivity and T is the absolute temperature.

However, It is possible that the efficiency could be improved by using a TEG module with higher $(ZT)_M$value (0.7–1) [42].

It is assumed for simplicity that the heat supplied on the hot side of the TEG is equal to the heat transferred due to the coolants. By substituting equations (4.2), (4.4), (4.5) and (4.19) in equation (4.21) and rearranging gives

$$(\eta_{optical} \times I_{sol} \times C \times A_r) - [h_a A_r(T_r - T_{amb}) + h_a A_w(T_{C-ave} - T_{amb})] - [\sigma\varepsilon A_r(T_r^4 - T_{amb}^4) + \sigma\varepsilon A_w(T_{C-ave}^4 - T_{amb}^4)](1 - \eta_{TEG}) = \frac{T_r - T_{cf}}{R_t} \quad (4.24)$$

A program loop is described in Figure 4.3 for solution the transient problem to predict T_r. The initial and boundary conditions of the system ingredients and ambient conditions are necessary to be input in the numerical modelling before the numerical iteration running. At the first, the values of T_r, is initially is assumed to be equal to the bulk temperature T_f, After many iterations the new values of T_r is usually determined by using equation (4.21). After determining Tr the electrical efficiency of the system, the electric output power, voltage output and current output can be calculated by estimating the temperature difference against the hot side and cold side temperatures of TEG as shown in Equations below.

$$T_h = T_r - \dot{Q}_d R_{1-2} \quad (4.25)$$

$$T_c = T_h - \dot{Q}_d R_{teg} \quad (4.26)$$

$$\Delta T_{teg} = T_h - T_c = \dot{Q}_d R_{teg} \quad (4.27)$$

After calculating $T_h and\ T_c$ the voltage (V), the output power, circuit current (I) and maximum current power point (Impp) at maximum point power (MPP) can be determined as the following.

$$P_{teg} = \eta_{TEG} \Delta T_{teg} \tag{4.28}$$

$$V_{oc} = NmS\Delta T_{teg} \tag{4.29}$$

$$V_{mpp} = \frac{R_o V_{oc}}{(R_o m R_i)} \tag{4.30}$$

$$I_{mpp} = \frac{P_{teg}}{V_{mpp}} \tag{4.31}$$

Where N is the overall number of thermo-element legs, m is the number of thermoelectric cells, R_i is the internal resistance of selected cell and R_o is the external load resistance.

The electrical efficiency η_{Elec}, of the system can be demonstrated as the ratio of the generated power and the overall of solar energy incidence on trough collector by the following equation [43].

$$\eta_{Elec} = \frac{P_{teg}}{I_{sol} \times A_{TE}} \tag{4.32}$$

The thermal energy gained by the collector with the solar radiation Isol can be utilized to estimate the mean thermal efficiency system.

$$\eta_{Th} = \frac{\dot{Q}_f}{I_{sol} \times A_{Thermal}} \tag{4.33}$$

The overall efficiency of system can be expressed as

$$\eta_{total} = \eta_{th} + \eta_{ele} \tag{4.34}$$

The percentage increase of CTEG-nanofluid electrical efficiency (percentage of the enhancement) relative to CTEG-water can be expressed as

$$\%\eta_{ele} = \frac{\eta_{ele-nano} - \eta_{ele-w}}{\eta_{ele-w}} \quad (4.35)$$

Where $\eta_{ele-nano}$ and η_{ele-w} are the electrical efficiencies ($\%\eta_{ele}$) of CTEG-nanofluid and CTEG-water respectively.

By the same manner, the percentage increase of CTEG-nanofluid thermal efficiency (percentage of the enhancement) relative to CTEG-water can be expressed as:

$$\%\eta_{th} = \frac{\eta_{th-nano} - \eta_{th-w}}{\eta_{th-w}} \quad (4.36)$$

Where $\eta_{th-nano}$ and η_{th-w} are the thermal energetic efficiency of CTEG-nanofluid and CTEG-water respectively.

4.6. ASSUMPTIONS FOR MODELLING

There are some basic assumptions for the computation of the model:

- The TEG supposed to be as one solid material, so that; the thermal characteristics of the structure and internal material are all ignored. The value of thermal resistance value that utilized in the model is calculated from the experimental test.
- Electrical resistivity, thermal conductivity and Seebeck coefficient of thermoelectric generator are not variable with temperature.
- The heat removed from thermoelectric cold side is supposed to be equal to full heat that being taken away by the coolants.
- The average temperature of the cooling fluid is equal to the average surface temperature of the cooling duct.

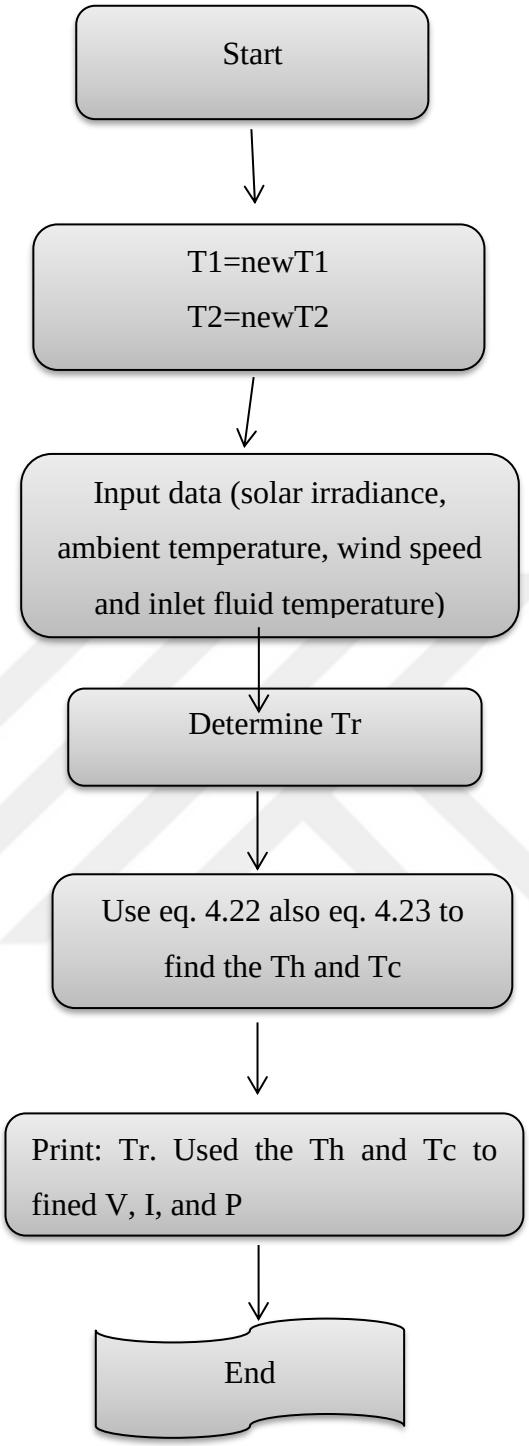

Figure 4.4. Flow chart of a computer program

CHAPTER 5

RESUTLS AND DISCUSSIONS

5.1. TESTING PROCEDURE

In this experimental study, many experiments were conducted at Karabuk University, Karabuk, turkey during the months of August September, after that, the steady days with the best weather circumstances were chosen in order to analyse their measurments. From 9:30 am to 5:00 pm the experiments were conducted daily for all the coolants which were pure water, graphene nanofluid and MWCNTs nanofluid, The parameters measured such as inlet and outlet coolants temperatures, thermoelectric surface temperature, solar irradiance, voltage and current were recorded simultaneously with constant flow rate adjusted at 0.5 L/min and 1L/min during the time of the experiment. Then, the data recorded for the selected days were averaged and utilized in computations as shown in table 5.1.

Table 5.1. Experimental for the selected coolants.

coolants	Number of experiment	Flow rate
Pure water	2	0.5L/min
Pure water	2	1.0L/min
MWCNTs nanofluid- 0.25wt	2	0.5L/min
MWCNTs nanofluid- 0.50wt	1	0.5L/min
Graphene nanofluid- 0.25wt	1	0.5L/min
Graphene nanofluid- 0.50wt	1	0.5L/min

5.2. NANOFLUID THERMAL PROPERTIES

Thermal characteristics for the selected nanofluids under investigation are evaluated by Eqs. 3.1-3.4 and illustrated in Table 5.1.

Table 5.2. Thermo physical of nanofluid

Nanofluids	**Wt %**	$\boldsymbol{\rho}$ $(\boldsymbol{kg/m^3})$	$\boldsymbol{k}$ $\boldsymbol{W/(m.K)}$	$\boldsymbol{Cp}$ $\boldsymbol{kJ/(kg.K)}$
MWCNT-Water	0.25	1091	0.9431	3.4063
MWCNT-Water	0.50	1185	1.4327	2.7531
Graphene-Water	0.25	1128	0.524	3.4126
Graphene-Water	0.50	1259	1.1755	2.803

Up to date, the thermal characteristics of nanofluids that have been measured experimentally and those that have been predicted by theoretical models currently differ significantly.

For small concentrations Eq. (3.1) Maxwell model is designed for continuous isotropic homogeneous material. [44]. In their experimental study over the thermal characteristics of oil heat transfer for MWCNT, Pakdaman et al. [45] sumed up that whereas the Xuan and Roetzel model results depart from the experimental data by a maximum of 22%, the Maxwell model results diverge from the measured values by a maximum of 13%. Phuoc et al. [46] estimated the thermal conductivity over o.5wt%MWCNT distilled water nanofluid.

5.3. RESULTS AND DISUSSIONS

The data measurements were collected continuously and simultaneously in each other 20s from the period of time from 9.30 am to 5.0pm, at 0.5L/min and 1.0 L/min flow rates for the coolants under investigation.

In case of the pure water, the experimental test was operate with 0.5L/min and 1.0 L/min flow rates for studying the influence of changing water flow rates on the CTEGsystem performance in order to make compromise with the MWCNTs nanofluids and graphene nanoplatelets distilled water at the same flow rates. After that, due to of having afew clear days of steady state weather circumstances, for all experiments the processes is changed to the costant flow rate of 0.5L/min. In order to cool the working fluid the city water is used of a 50 liters storge tank combied with

the copper coil heat exchanger at L/min flow rate, after that, the days eith the best steady state weather terms and clean were selected to be used in the analysis.

5.3.1. Distilled Water Experiments

For pure water two days with steady state weather terms were choosen, which are 10^{th} and 26^{th} of August for the flow rates of 0.5 L/min and 1.0 L/min respectively.

Figure 5.1and figure 5.2 show the measured parameters on the selected days continuously, which were clear days with steady state conditions nevertheless some passing light clouds in the second test at noon time. After that, the measured parameters were averaged and discussed in details. For the flow rate of 0.5 L/min date of 10^{th} of August the mean solar radiation and ambient temperature over the test period for the selected day were 839.6 W/$m^2$and 34.6 °C respectively. The average measured hot side surface temperature was 59.7 °C and the cold side surface temperature was 31.8°C.

In addition, the second testing day was in 26^{th} of August for the flow rate of 1.0 L/min where some clouds passed for short time in the sky at the evening period, which directly influences the current, voltage and thermoelectric generator hot side temperature. The determined average solar radiation and average ambient temperature during the test day of the experiment were 826 W/m² and 32.6℃ respectively. The average hot and cold side temperatures were 59.2 °C and 31.1°C respectively, whereas the inlet and outlet fluid temperatures the average values of 24.9°C and 26.4°C were achieved.

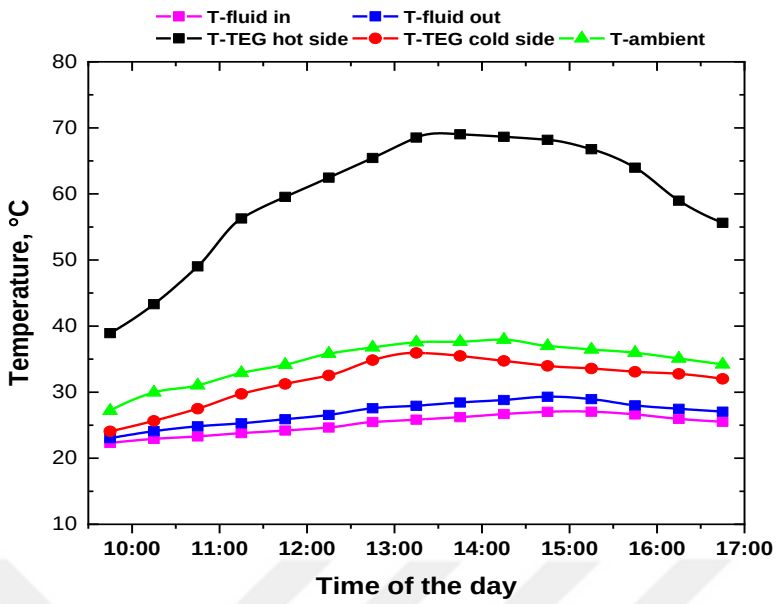

Figure 5.1. Daily measured parameters for pure water at flow rate of 0.5L/min.

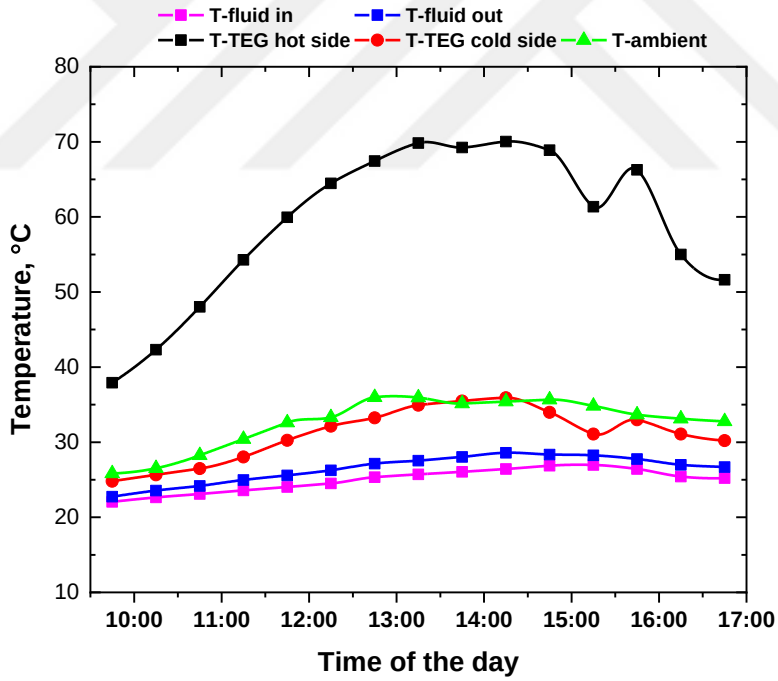

Figure 5.2. Daily measured parameters for pure water at flow rate of 1.0L/min.

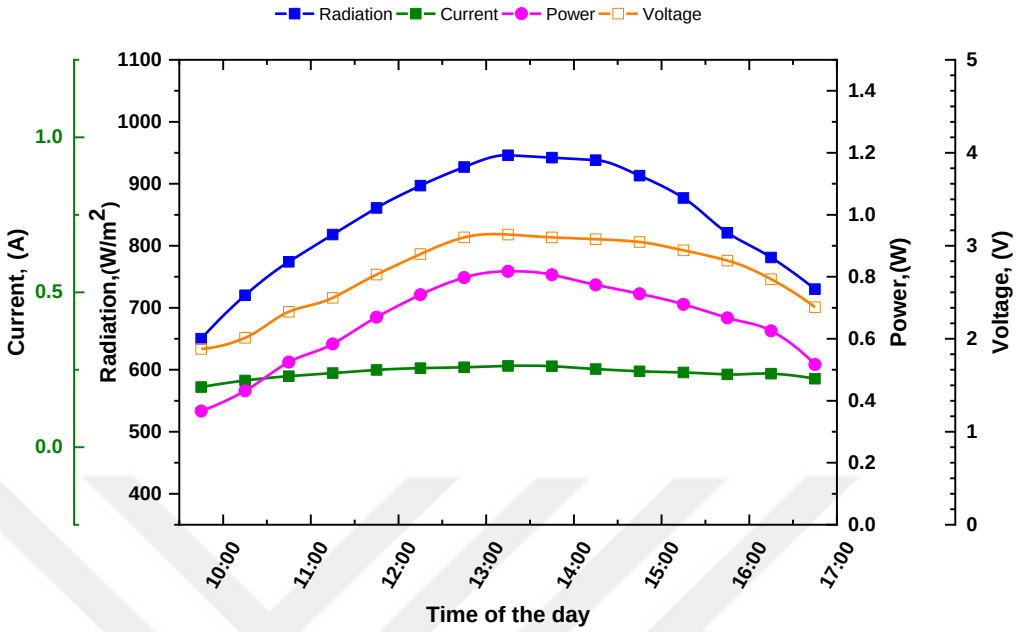

Figure 5.3. Daily measured and estimated parameters for pure water at 0.5L/min.

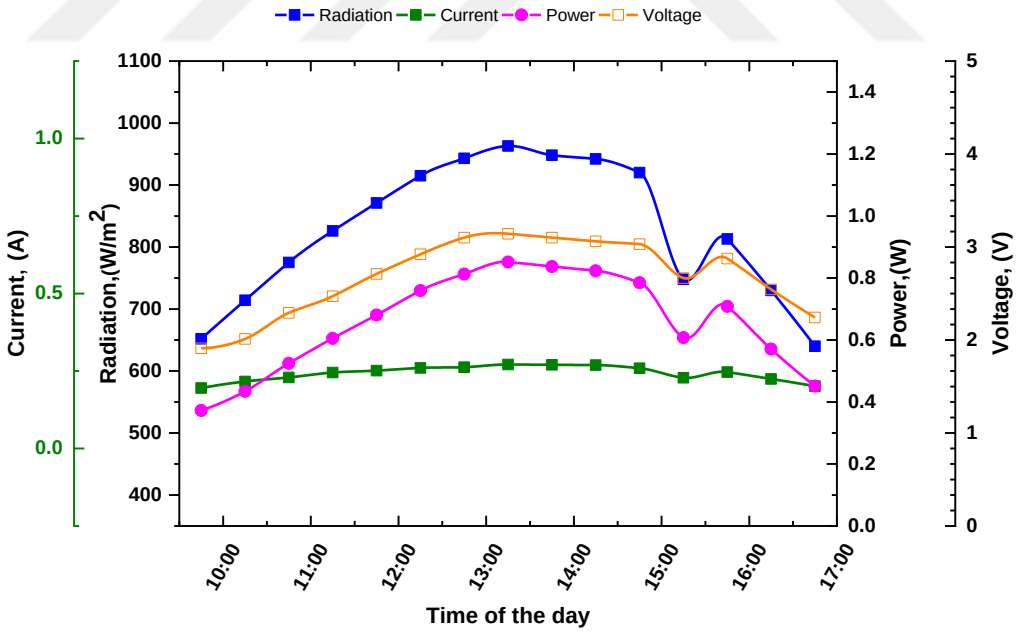

Figure 5.4. Daily measured and estimated parameters for Pure water at 1.0L/min.

Figure 5.3 and Figure 5.4 explain the fluctuations of voltage and current of CTEG system at 0.5 and 1.0 L/min flow rates respectively. From these figures, we can observe the generated voltage and current of the system in the case of 0.5 L/min flow

increased by 0.75% and 0.78% relative to pure water at flow rate of 1.0 L/min. For 1.0 L/min case the generated voltage and current during the test day are 2.67V and 0.24 A respectively. The electrical power generated at different flow rates also depicted in previous figures. It can be seen that the electrical power for 0.5L/min is very close from that generated by 1.0 L/min because of the cooling and solar radiation effects. Moreover, the produced power by CTEGs at flow rates 0.5 L/min and 1.0 L/min at the peak period are 0.73 W and 0.72 W respectively. Moreover, it is obvious from the figures that the generated electrical output power does not have a big answer to change of water flow rate.

In order to get a clear comparison between the variation of flow rate at 0.5L/min and 1.0 L/min, the data collected of the weather circumstances (ambient temperature and radiation), hot and cold surface temperature of thermoelectric, and estimated electrical efficiency were averaged for the experiment interval (9:30–17:00) and for the peak interval of radiation (11:15–15:45) and abstracted in tables 5.3 and 5.4 respectively.

Table 5.3. Average daily measured and calculated parameters for pure water during the experiment interval (9:30 - 17:00).

Coolant	I_{sol}	T_{amb}**(°C)**	Th **(°C)**	Tc **(°C)**	V **(v)**	P **(W)**	η_{ele}(%)
Pure water at 0.5 L/min	839.6	34.6	59.7	31.8	2.69	0.65	4.69
Pure water at 1.0 L/min	826	32.6	59.24	31.1	2.67	0.645	4.73

Table 5.4. Average daily measured and calculated parameters for pure water during the experiment interval (11:15 - 15:45)

Coolant	I_{sol}	T_{amb}(°C)	Th (°C)	Tc (°C)	V (v)	P(W)	η_{ele}(%)
Pure water at 0.5 L/min	894	36.2	64.88	33.5	2.92	0.73	4.95
Pure water at 1.0 L/min	887	34.2	65.3	32.9	2.90	0.72	4.91

5.3.2. Experiments of 0.25 wt% Nanofluids

For the MWCNT nanofluid case Fig. 5.5, at afternoon time the weather changed to cloudy and partly windy for short time, which directly affected the current, voltage and the hot side temperature of the thermoelectric generator whereas, the inlet and outlet fluid temperatures of MWCNT nanofluid distilled water were not influenced because of a small time was not enough for the experiment to solar irradiance sudden variations. At noon time, the mean surface temperature of the hot side of TE was 68.27 °C, while the average surface temperature of the cold side of TE was 33 °C at maximum solar radiation of 956 W/m^2 and ambient temperature of 34 °C.

In case of graphene nanoplatelets nanofluid distilled water Fig. 5.6, where the steady state of weather condition most of the day and the hot surface temperature for the TE increased gradually from 37.8℃ at 09:30 to 73.4℃ at 13:45, respectively, which progressively decreased until 17:00 recording the value of 56.7℃. At noon, the average measured TE cold surface temperature was 22.7°C at9.30 to 34.9℃ at 13.45 respectively. The determined average solar radiation and average ambient temperature during the test day of the experiment were 853 W/m² and 27.6℃. The maximum value in the difference in surface temperature between the hot and cold sides with graphene nanoplatelets nanofluid is 38.4℃ at maximum value of solar radiation of 1014W/m².

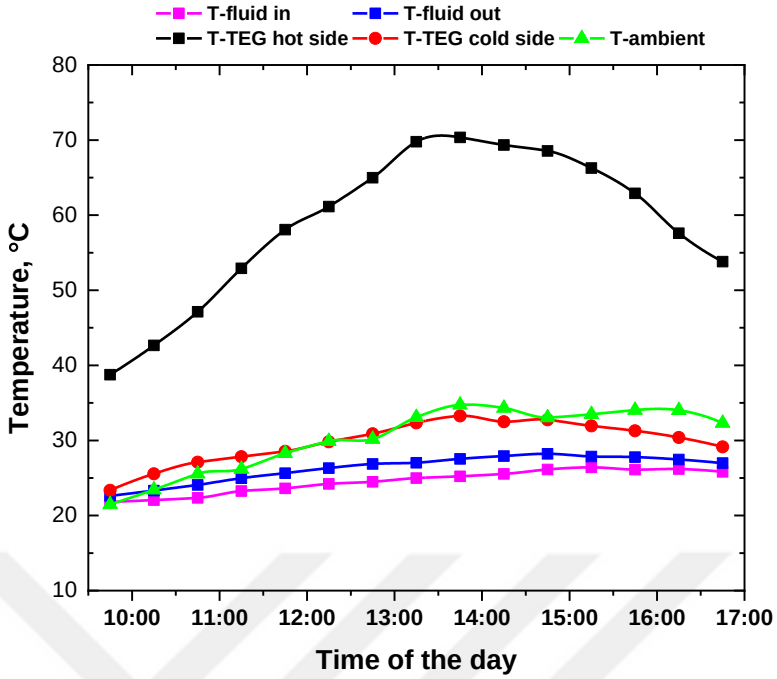

Figure 5.5. Daily measured parameters for MWCNT 0.25 wt%.

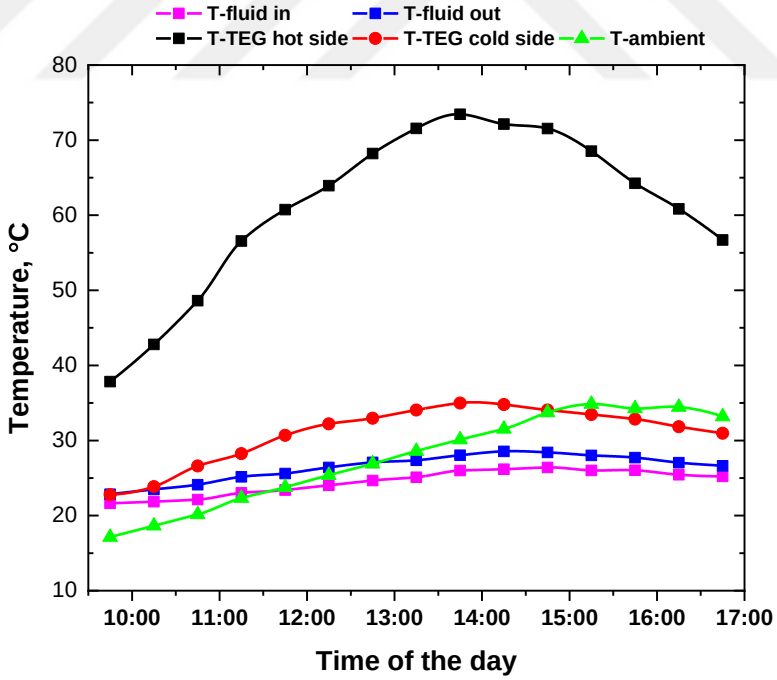

Figure 5.6. Daily measured parameters for Graphene 0.25 wt%.

In the figures 5.7 and 5.8, the changing of electrical output power generated by CTEG system follow up the same path of solar irradiance during the test interval, in

which at maximum solar radiation the maximum electrical power could be generated, where the maximum electric power for MWCNT nanofluid and graphene nanoplatelets nanofluid 0.83(W), 0.90(W) for a single thermoelectric generator respectively. The maximum generated current and voltage are 3.23V and 0.28A with the solar radiation of 1014W/m^2 for the Graphene nanoplatelets and the maximum generated current and voltage for the MWCNT-water are 3.15Vand 0.26A at the highest solar ration of 958 W/m^2 respectively.

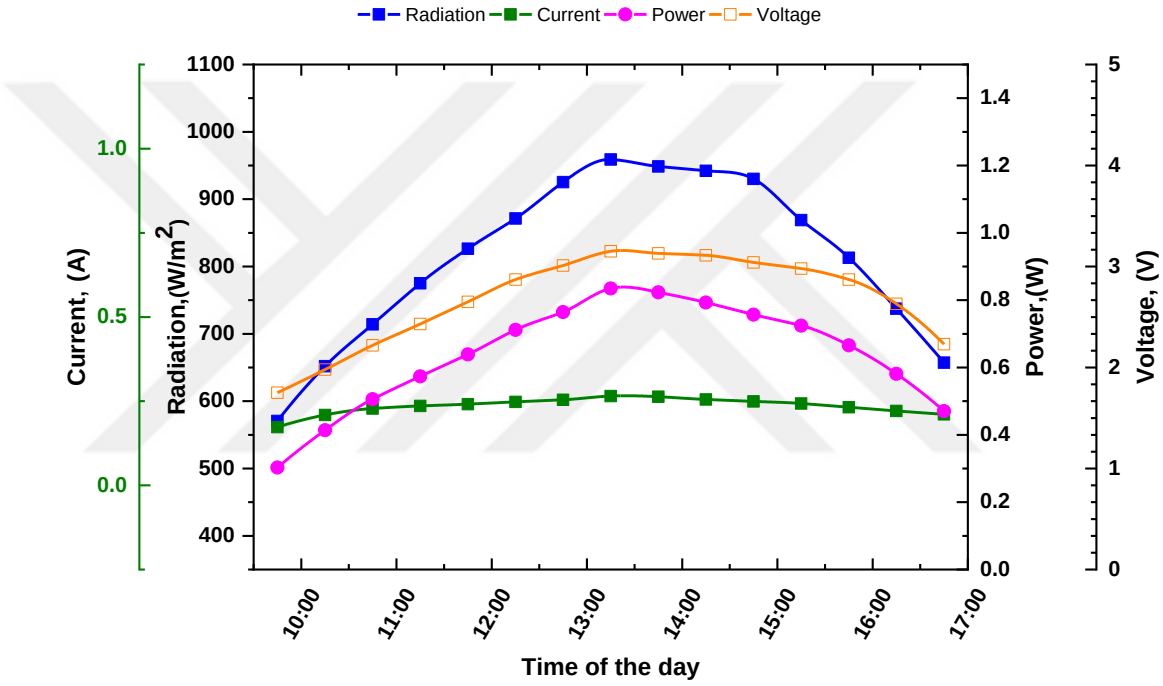

Figure 5.7. Daily measured and calculated parameters for MWCTs 0.25wt%

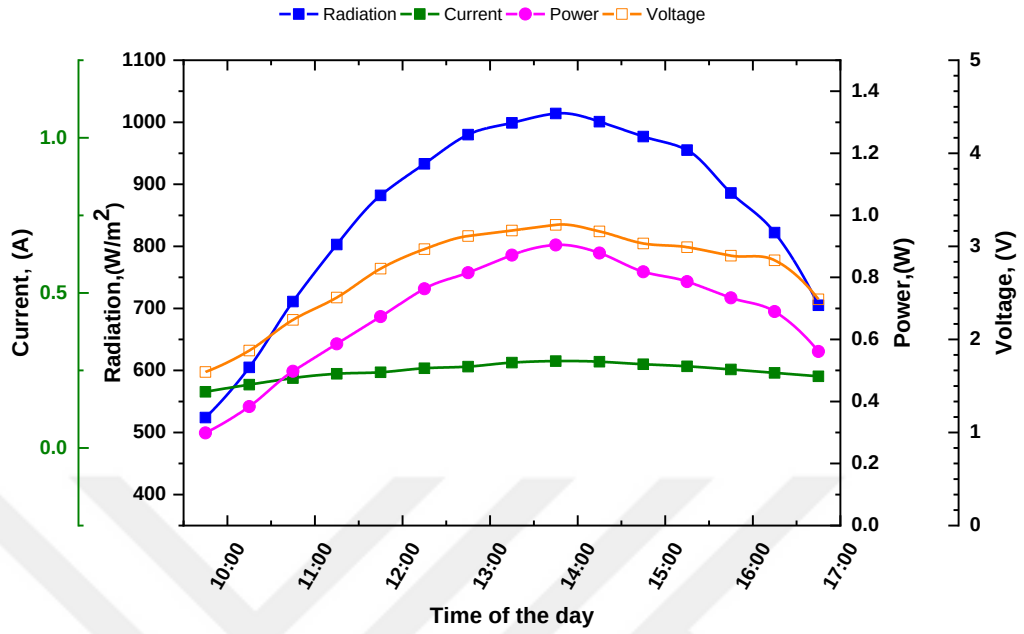

Figure 5.8. Daily measured and calculated parameters for garaghene 0.25wt%

In order the selected coolants obtain a well comparison ,the data collected of weather circumstances such as solar radiation, ambient temperature, hot side temperature of thermoelectric and estimated electrical efficiency were averaged for the test interval (9.0-17.0and for the peak time of (11:15–15:45) and listed in Tables 5.3 and 5.4, respectively.

Table 5.5. Average daily measured weather conditions, for MWCNT nanofluid graphene nanoplatelets nanofluid during the experimental time of (9:30 – 17.0)

Coolant	I_{sol}	T_{amb}(°C)	Th (°C)	Tc (°C)	V (v)	P (W)	η_{ele}(%)
water	839.6	34.6	59.7	31.8	2.69	0.65	4.69
Graphene 0.25wt%	853.1	27.6	61.2	30.9	2.72	0.68	4.83
MWCNT 0.25wt%	812	30.2	58.9	29.7	2.67	0.63	4.70

Table 5.6. Average daily measured weather conditions, for or MWCNT nanofluid graphene nanoplatelets nanofluid during the experiment period (11:15 - 15:45)

Coolant	I_{sol}	T_{amb}(°C)	Th (°C)	Tc (°C)	V (v)	P(W)	η_{ele}(%)
Water	894	36.2	64.88	33.5	2.92	0.73	4.95
Graphene 0.25wt%	943	29.1	67.0	32.8	2.97	0.78	5.01
MWCNT 0.25wt%	885	31.7	64.4	31.1	2.92	0.72	4.93

As illustrated in Tables 5.3 and 5.4, the following observations can be done. First of all, there is an agreement in the results of the electrical efficiency for pure water obtained by Fan [10]. Secondly, cooling thermoelectric module with liquid working fluid decrease the maximum cell temperature and then the electrical efficiency increased. As a result, the 0.5 wt% MWCNTs nanofluid state showed up better stability in electrical efficiency than graphene nanoplatelets nanofluid and pure water. As shown in Figure.5.9, MWCNT nanofluid is the most electrically efficient fluid coolant as compared to rest of the coolants

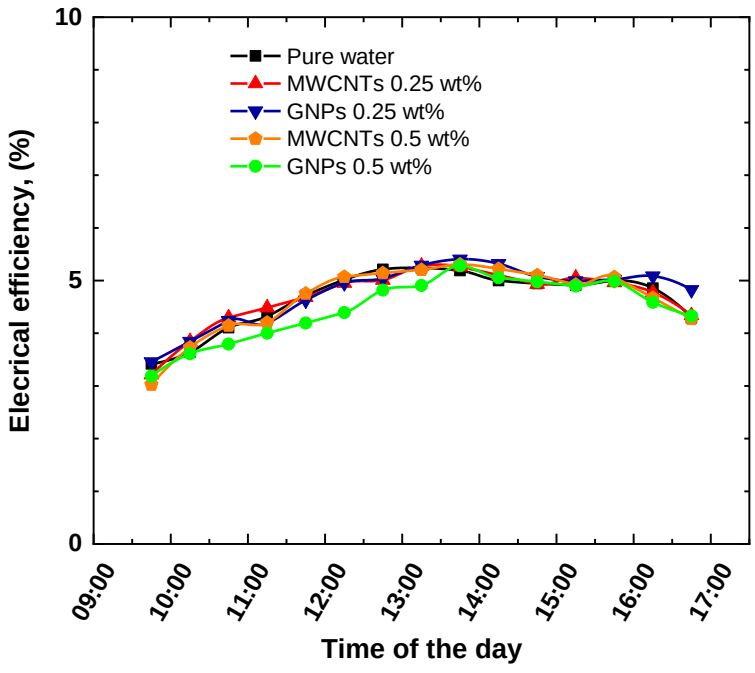

Figure 5.7. Daily averaged electrical efficiency for flow rate of 0.5 L/ min.

5.3.3. Experiments of 0.5 wt% Nanofluids

For the nanofluids with 0.5wt% concentration more experiments have been done in order to collect more data. The nanofluids tests conducted in the period of 23Sep and 03Oct.2019 at constant 0.5 L/min flow rate. Both of MWCNT and graphene nanoplatelets distilled water nanofluids the concentration of 0.5 wt% is prepared by additional a confirmed weight of pure water based on the instructions of the manufacturer.

For the MWCNT nanofluid case, as shown in Figure 5.10 the sky was clear with steady state weather conditions. Over the days of experiments, the average solar irradiance and ambient temperature for MWCNT water-based nanofluids were 803.4 W/m², 29.5 °C respectively, while, the average measured of hot surface temperature was 58.8 °C.

For all cases of selected coolants, at about two hours before noon, the maximum difference between hot and cold surface temperatures can be achieved. This occurs because; at morning, the hot surface temperature is lower as a result of lower solar irradiance and temperature of the coolant. As solar radiation increases, the surface temperature difference of TE increases because the hot surface temperature of TE generator increases. As time passes, the difference of surface temperature continues increasing until reaching the maximum point.

For the Graphene nanofluid figure 5.11, the testing day was in the 3th of October, where some clouds appeared for short period in the sky at the morning and afternoon intervals, which directly influences the current, voltage, thermoelectric generator hot side temperature whereas, nanofluid inlet and outlet temperatures were not affected because there was not enough time for the system to follow the solar radiation sudden fluctuations. Over the day of the experiment, the average surface temperature of the hot side of TE was 58.2 °C, while the average surface temperature for the cold side of TE was 30.4 °C, whereas, average solar irradiance and ambient temperature were 757W/m2 and 27 °C respectively.

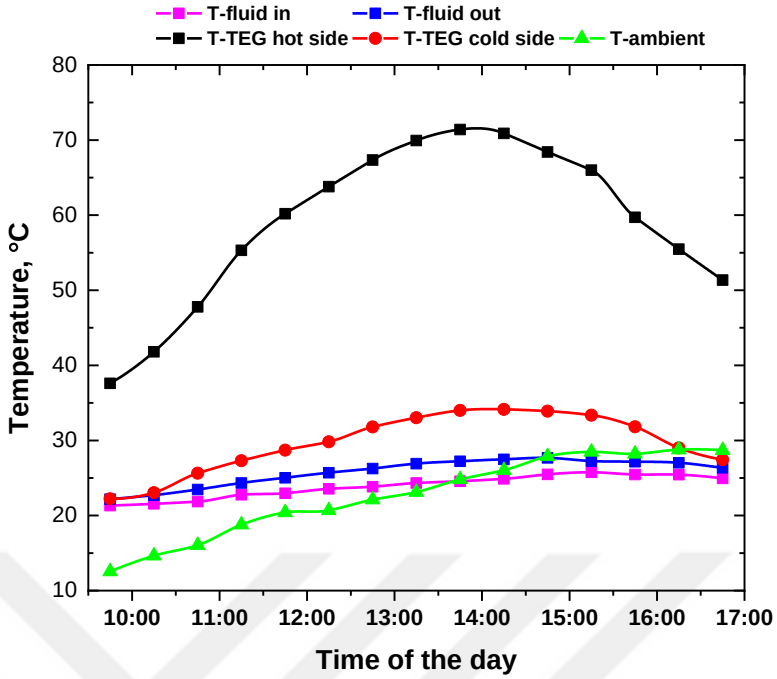

Figure 5.8. . Daily measured parameters for MWCTs 0.50wt.

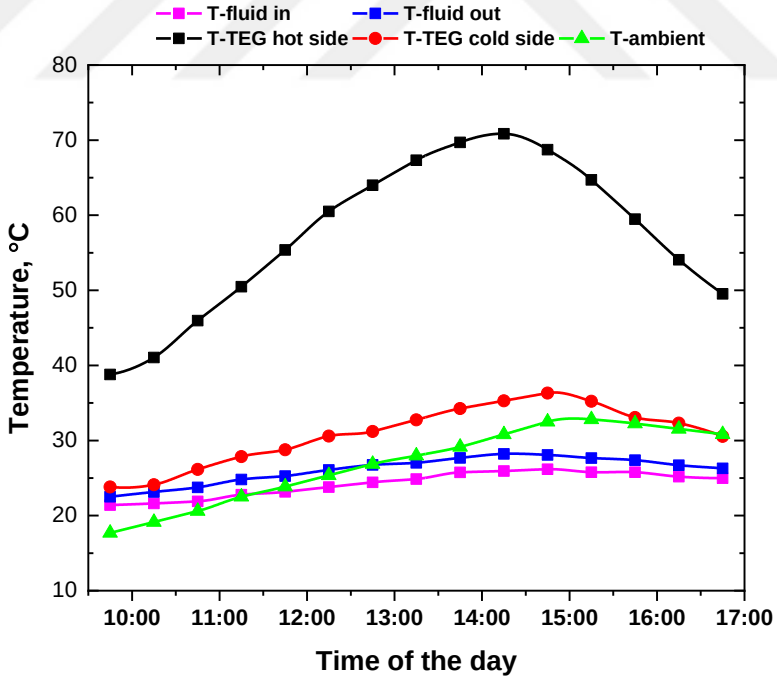

Figure 5.9. . Daily measured parameters for Graphene 0.50wt.

Figures, 5.12 and 5.13. Show the variation of voltage and current of the CTEG at 0.5L/min flow rate for the selected coolants. From these figures, the average

generated current, voltage and generated power for the MWCNT nanofluid were 0.239A, 2.649Vand 0.63W respectively, whereas, for the Graphene nanoplatelets nanofluid there was some sudden changes in the weather at the beginning of the experiment due to some passing clouds as shown in Figure 5.13. These changes in solar radiation directly affected the generated voltage, current and the hot surface temperature of thermoelectric module, while the temperatures of the coolant were not influenced due to insufficient time for the coolant to interact to these sudden changes. The average generated current, voltage and generated power were 0.229A, 2.509V and 0.58 respectively. It can be observed that the current, voltage and generated electrical power for MWCT are higher than the Graphene case because of the effect of solar radiation.

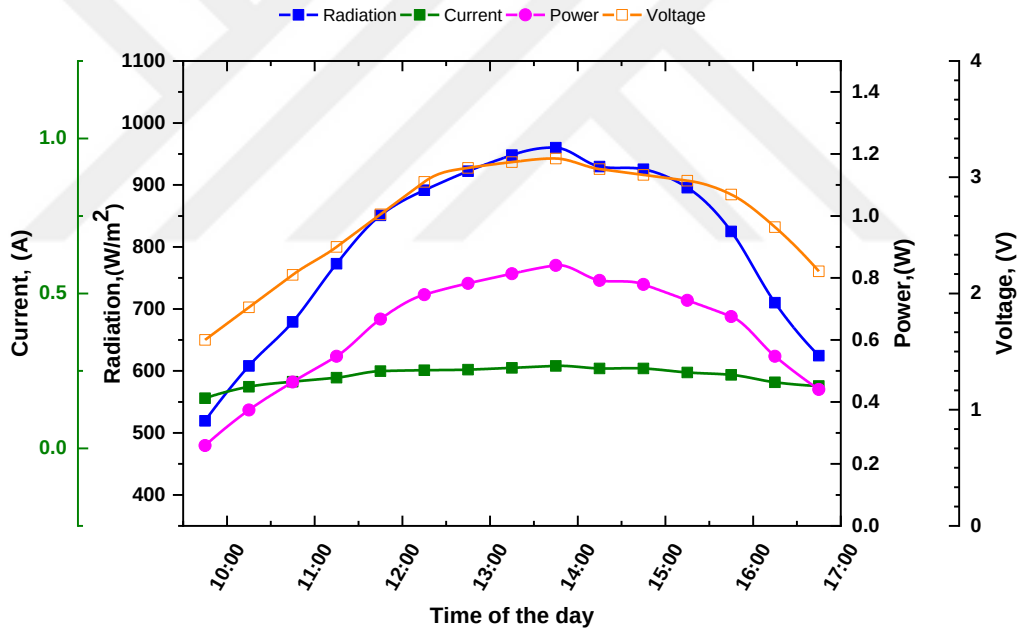

Figure 5.10. Daily measured and calculated parameters for MWCTs 0.50 wt%.

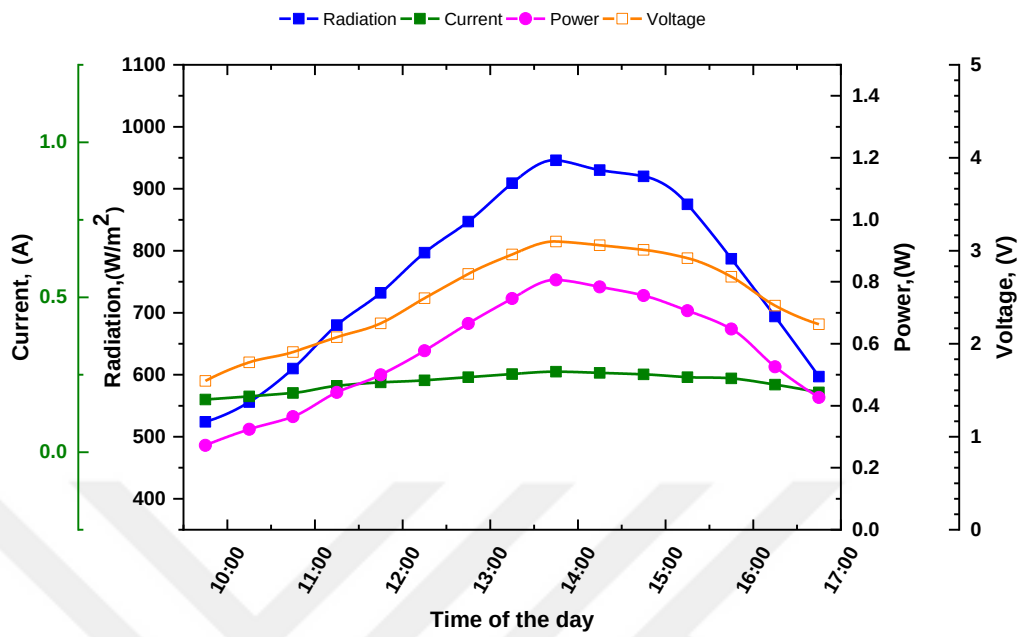

Figure 5.11. Daily measured and calculated parameters for Graphene 0.50 wt.

To investigate a clear comparison between the selected coolants, the data collected of weather circumstances like, thermoelectric hot side temperature and evaluated electrical efficiency were averaged for the experiment interval of (9:30–17:00) and for the peak interval of solar radiation (11:15–15:45) and summarized in Tables 5.7 and 5.8, respectively.

Table 5.7. Average daily estimated weather conditions, for MWCNT nanofluid graphene nanoplatelets nanofluid during the experiment interval (9:30 - 17:00).

Coolant	I_{sol}	T_{amb}(°C)	Th (°C)	Tc (°C)	V (v)	P (W)	η_{ele}(%)
Graphene 0.5wt%	775	25.7	58.2	29.4	2.50	0.58	4.42
MWCNT 0.5wt%	803	22.7	59.9	30.5	2.64	0.63	4.65

Table 5.8. Average daily estimated weather conditions, for MWCNT nanofluid graphene nanoplatelets nanofluid during the experiment interval (11:15 - 15:45)

Coolant	I_{sol}	T_{amb}(°C)	Th (°C)	Tc (°C)	V (v)	P(W)	η_{ele}(%)
Graphene 0.5wt%	841	28.3	63.31	32.4	2. 73	0.66	4.75
MWCNT 0.5wt%	891	24.04	64.90	31.5	2.93	0.73	4.99

From Table 5.7 and Table 5.8, MWCNTs nanofluid showed a better in output power, voltage and electrical efficiency than graphene nanoplatelets nanofluid water.

5.4. THERMAL AND OVERALL EFFICIENCIES

As mentioned before, the value of energy which can be extracted from the trough collector can be explaining by the thermal efficiency, so the overall efficiency of the CTEG can be calculated by Eq. 4.33.

Total efficiency is influenced by electrical efficiency less than thermal efficiency. The thermal efficiency fluctuations entire the test of the experiment does not track a specific trend, as a result of experimental conditions variations such as ambient temperature, humidity, wind velocity and the amount of solar radiation as shown in figures 5.14 and 5.15. Table 5.7 describes the daily average thermal and total efficiencies for the selected coolants. Because of its relatively higher heat capacitance (ρ ×Cp), the experimental outcomes showed that graphene nanoplatelets distilled water showed better in thermal efficiency and consequently the overall efficiency than MWCNT nanofluid and pure water. As a result, for the 0.25 wt% the averages of the daily overall efficiency for the day-long periods were 18.69%, 19.87% and 18.91% for distilled water, graphene and MWCNT respectively, whereas during the peak period the averages of the daily overall efficiency were 19.78%, 20.14% and 19.82% for distilled water, graphene and MWCNT respectively. Moreover, for the 0.5 wt% the averages of the daily overall efficiency for the day-long periods were 19.54% and 18.18% for graphene and MWCNT respectively, whereas during the peak period the averages of the daily overall

efficiency were 18.87% and 19.36% for MWCNT nanofluid and graphene nanoplatelets nanofluid respectively.

Table 5.9. Daily average thermal and overall efficiencies.

Coolant	**(9.30-17)period**		**(11.15-15.45)period**	
	Thermal Eff. (%)	Overall Eff. (%)	Thermal Eff. (%)	Overall Eff. (%)
Pure water	14.00	18.69	14.83	19.78
Graphene - 0.25 wt%	15.04	19.87	15.13	20.14
MWCNT- 0.25 wt%	14.21	18.91	14.89	19.82
Graphene - 0.5wt%	15.12	19.54	14.61	19.36
MWCNT- 0.5 wt%	13.53	18.18	13.88	18.87

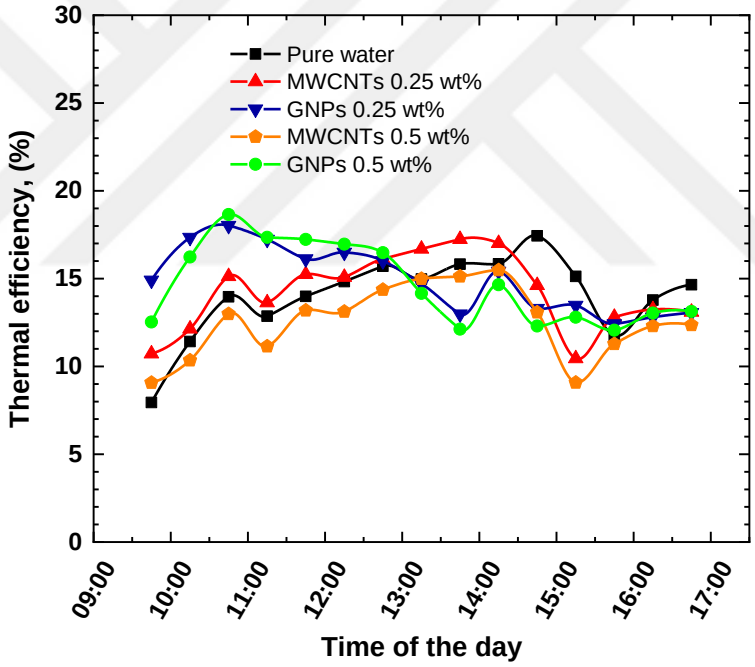

Figure 5.12. Daily averaged variations of the thermal efficiency for the selected coolants for wt 0.25% and 0.5L/min.

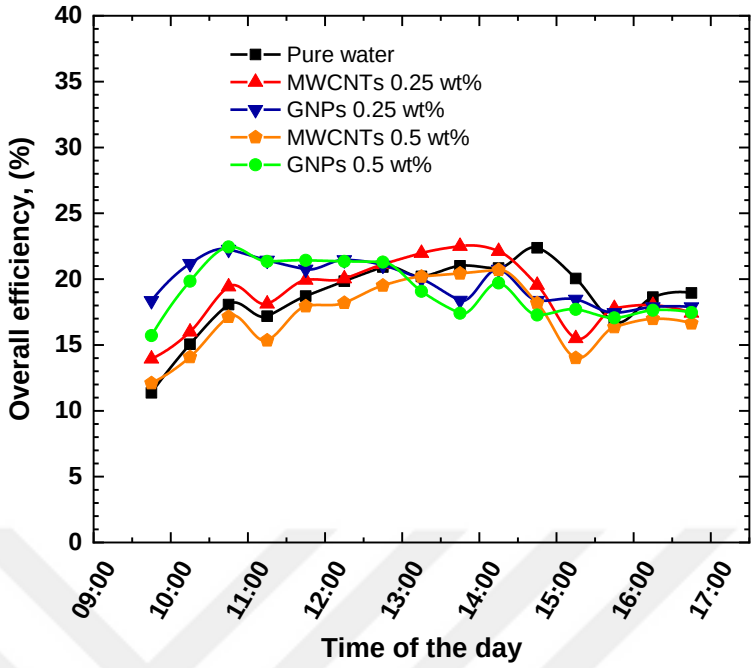

Figure 5.13. Daily averaged variations of the overall efficiency for the selected coolants

5.5. NUMERICAL MODEL VALIDATION OF CTEG SYSTEM

The implemented mathematical modelling can be used to estimate the power output and some other parameters including the thermal and electric efficiencies of the system. The simulation was conducted using MATLAB software in case of pure water with flow rate of 0.5 L/min and several runs were conducted in order to validate the experimental results. Figures (5.16, 5.17, 5.18) show the model validation with various terms. It can be observed that there is an agreement between the experiment and estimated values and moving in the range of ± 14 %.

Appendix tables show the validation of the modelling results with different experimental conditions. It observed that the agreement between the experiment and evaluated values are in good agreements. Figure 5.16 shows the temperature profiles of the system at various solar radiations. It is observed that the prediction of the output fluid temperature is less than the experimental values where the theoretical value is 0.7% lower. For the hot side temperature, the numerical model had predicted ~21% higher than the outdoor results while, for the cold side temperature the

experimental results had predicted 3.4% lower than the numerical model. The TEG cold side temperature is gradually increased compared to the average variation of the hot side temperature.

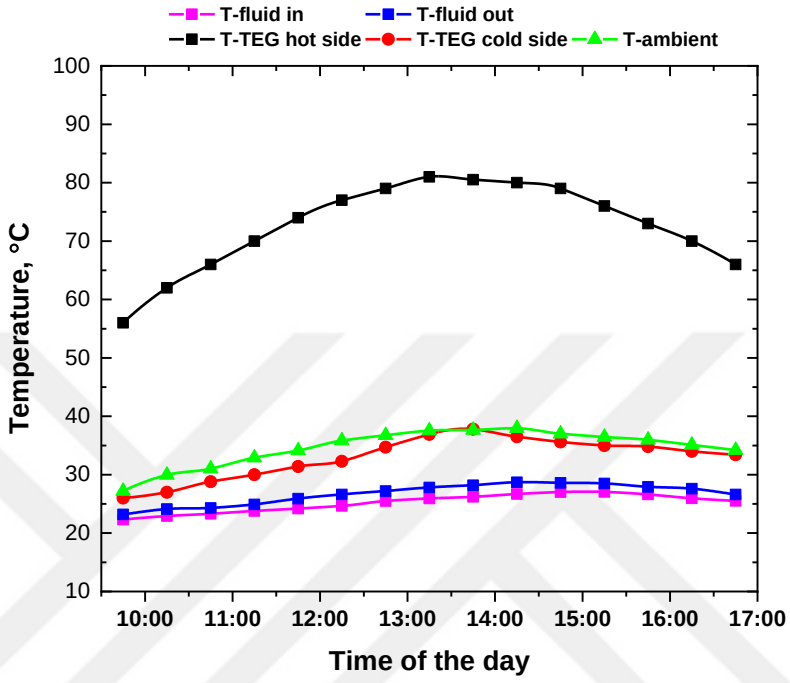

Figure 5.14. Temperature profile for pure water at 0.5 L/min

Figure 5.17 presents the predicted power output, voltage and current at the given solar radiations. As for the electrical prediction for the system, there were small disagreement between the numerical and the current outdoor results. For the outputs power, the numerical model had predicted ~20% higher than the outdoor results. For the voltage the predicted result is ~4.8% higher than the outdoor results. For The generated current the numerical values had evaluated 16% higher. One of the causes of the difference between theoretical and experimental results is due to this experimental tests didn't take many various parameters into account so other parameters still need to be investigated such as wind parameter, reflectivity, the flatness of the reflecting material as well as experimental errors.

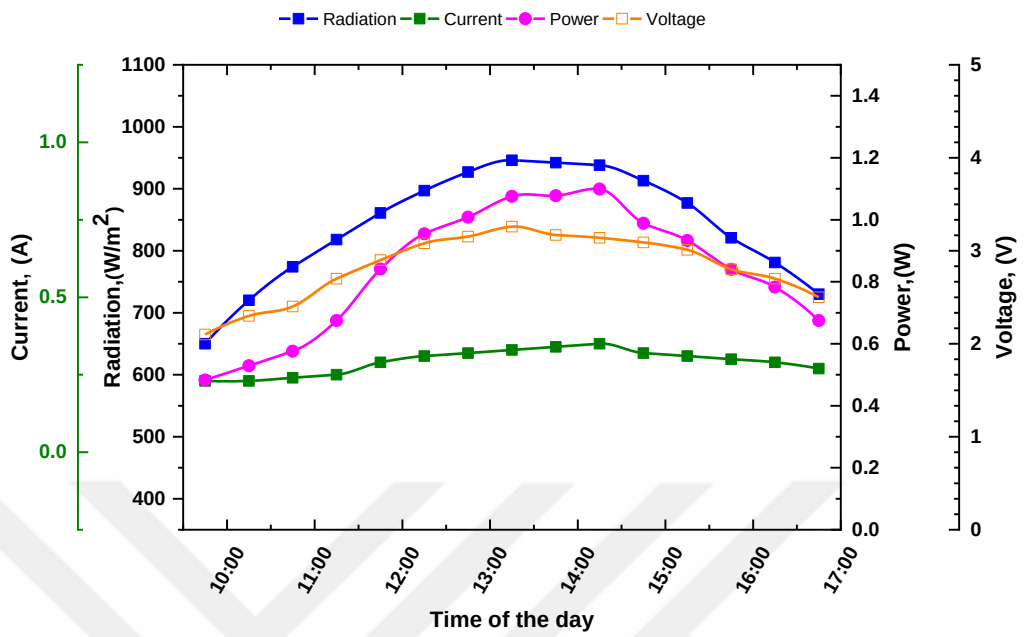

Figure 5.15. Power outputs validation for pure water at 0.5 L/min

Table 5.10 shows the average electrical and thermal results comparison for the all the parameters between outdoor experiments and numerical modelling.

Table 5.10. Validation results for pure water at 0.5 L/min.

Parameter	outdoor	modelling	difference
Output fluid temperature (℃)	26.86	26.67	0.70%
Hot side thermoelectric temperature Th (℃)	59.7	72.6	-21.7%
Cold side thermoelectric temperature Tc (℃)	31.80	32.9	-3.40%
Voltage (V)	2.69	2.82	-4.83%
Current (A)	0.24	0.28	-16.66%
Power output (W)	0.65	0.78	-20%
Thermal efficiency (%)	14	11.33	19%
Electrical efficiency (%)	4.69	5.95	-26%

The modelling results were approximately 20% and 5% higher on the power and voltage outputs than in the outdoor experiment. The power generation is controlled by the temperature difference against the TEG module, the two electrical results were expected to be lower because of the lower temperature difference against the TEG during the outdoor experiment.

Figure 5.18 shows the thermal and electrical efficiencies. For the electrical efficiency the numerical model was 5.95% which was 26% higher than the experimental model. The numerical thermal efficiency of the system was 11.33% which means the the numerical model had predicted ~19% higher than the outdoor results.

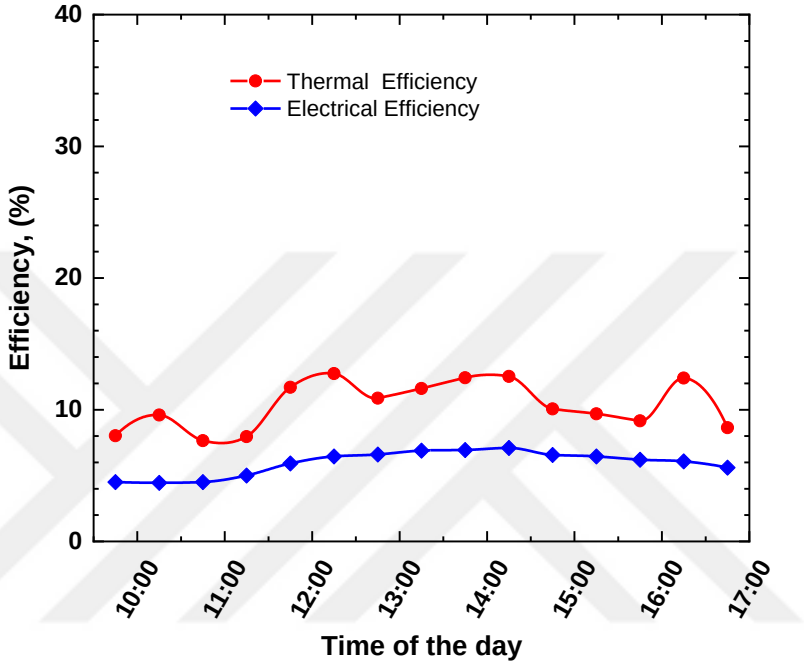

Figure 5.16. Electrical and thermal efficiencies results validation for pure water at 0.5 L/min.

CHAPTER 6

CONCLUSION

In this experimental and theoretical studies**, the** performance estimation of a system thermoelectric generator operated by pure water, graphene nanoplatelets distilled water nanofluid and MWCNTS distilled water nanofluid with the concentration of 0.25 wt% and 0.50 wt% were performed.

At the first the experimental study with the pure water of flow rates of 0.5 L/min and 1.0 L/min is conducted. During the period of experiment, the thermal outcomes of 0.5 L/min flow rate exams showed better in stability so that, it is chosen to be used in the all experiments.

According to the analysis conducted on the experiments of pure water of 0.5 L/min and 1.0L/min the following results can be summarized:

Utilizing the different of flow rate lead to increase in thermal efficiency more than the electrical efficiency. At 0.5L/min the mean average increment in thermal efficiency from14% to 15.6 at 1.0L/min flow rate, while average increment in electricall efficiency from4.69% to 4.74 at 1.0L/min flow rate.

The daily mean hot side surface temperature increasing as solar radiation increases. In case of 0.5 L/min flow rate, the daily mean hot surface temperature was 59.7 °C, while it was 59.2 °C in the case of 1.0 L/min flow rate.

According to the analysis conducted on the 0.5 wt% and 0.25 wt% nanofluids experiments, the following outcomes can be achieved:

In the thermal efficiency state, the graghene distilled water nanofluid showed higher than MWCNTs distilled water nanofluid. For the concentration of 0.25wt% the mean thermal efficiencies for graghene nanoplatelets stae and MWCNT case were 15.04% and 14.21% respectively.

In the electrical efficiency case, the graphene nanoplatelets pure water nanofluid showed up the better in stability than MWCNT-water nanofluids and pure water during the peak period of solar radiation.

The concentrator thermoelectric generator system (STEGs) designed and fabricated in this thesis was able to generate about 4.5 W electricity at the different in temperature of 38.4C° between hot and cold sides for Graphene nanofluid case, whereas, it could generated about 4.15 W at temperature difference of 36.7C° for the MWCNT-water nanofluids case.

For MWCNT nanofluid 0.25wt% state the electrical efficiency percentage increase was was 0.2% whereas it was 2.98% for graphene nanoplatelets nanofluids 0.25wt% state. Moreover, the mean percentage increase in thermal efficiency for 0.25 wt% graphene nanoplatelets nanofluids and 0.25 wt% MWCNT nanofluid were 7.4% and 1.5% respectively.

In case of 0.5 wt% graphene nanoplatelets nanofluid showed up better stability in thermal efficiency than MWCNT nanofluid and pure water. This stability of graphene nanoplatelets attribute to the high in thermal conductivity, which gives it the capacity to waste heat more than other coolants.

Due to influences in the parameters such as wind speed, flatness of the reflective material, different in reflectivity because of oxidation of the aluminum film, as well as error in tracking system make the actual efficiency is much lower .

Using theoretical models for evaluating the nanofluids thermal properties of makes the nanofluid thermal behaviour difficult to explain.

Since it is really hard to find steady weather conditions with clear days in karabuk city, it is highly recommended to conduct the test procedure of two separated parts of cooling ducts, with the same specification and trough collector in order to prove the influences of the coolants on the thermal behaviour, it gives the accuracy for the measurements.

6.1. RECOMMENDATION FOR FUTURE WORK

Using Carbon nanofluids, instead of MWCNT, such as graphene oxide and graphite in solar power systems in the literature still small, hence investigating the effects of utilizing these nanofluids in CTEG systems will be covered.

Since the trough collector system is driving force that supplied the thermal heat to the thermoelectric generators, which should be efficient and reliable. For future work mirror reflectors is strongly encouraged for system improvement.

The natural of heat transfer must be understood through the system, which in turn leads to improve the overall efficiency.

A developed mechanism of the heat transfer system must be founded also a well insulation in order to avoid the strong influence from the ambient fluctuation.

Utilizing a new thermoelectric material based on the nanometre engineering is strongly recommended to enhance the overall efficiency. Therefore, more collaboration with researchers who can utilize nano-thermoelectric material is strongly encouraged.

REFERENCES

1. IEA, I., "World energy outlook 2011", ***Int. Energy Agency***, 666: (2011).

2. Ten Hoeve, J. E. and Jacobson, M. Z., "Worldwide health effects of the Fukushima Daiichi nuclear accident", ***Energy & Environmental Science***, 5 (9): 8743–8757 (2012).

3. développement, P. des N. unies pour le, Unies, N., and l'énergie, C. mondial de, "World Energy Assessment: Energy and the Challenge of Sustainability", ***United Nations Development Programme***, (2000).

4. Makrides, G., Zinsser, B., Norton, M., Georghiou, G. E., Schubert, M., and Werner, J. H., "Potential of photovoltaic systems in countries with high solar irradiation", ***Renewable And Sustainable Energy Reviews***, 14 (2): 754–762 (2010).

5. Kalogirou, S. A., "Solar Energy Engineering: Processes and Systems", ***Academic Press***, (2013).

6. Tan, H., "The development and applicability of renewable energy for buildings", ***Build Sci***, 8: 34–42 (2015).

7. Rowe, D. M. and Min, G., "Evaluation of thermoelectric modules for power generation", ***Journal Of Power Sources***, 73 (2): 193–198 (1998).

8. Muthu, G., Shanmugam, S., and Veerappan, A. R., "Theoretical and experimental study on a thermoelectric generator using concentrated solar thermal energy", ***Journal Of Electronic Materials***, 48 (5): 2876–2885 (2019).

9. Shanmugam, S., Eswaramoorthy, M., and Veerappan, A. R., "Modeling and analysis of a solar parabolic dish thermoelectric generator", ***Energy Sources, Part A: Recovery, Utilization, And Environmental Effects***, 36 (14): 1531–1539 (2014).

10. Fan, H., Singh, R., and Akbarzadeh, A., "Electric power generation from thermoelectric cells using a solar dish concentrator", ***Journal Of Electronic Materials***, 40 (5): 1311–1320 (2011).

11. Li, Y., Wu, Z., Xie, H., Xing, J., Mao, J., Wang, Y., and Li, Z., "Study on the performance of TEG with heat transfer enhancement using graphene-water nanofluid for a TEG cooling system", ***Science China Technological Sciences***, 60: 1168–1174 (2017).

12. Ahammed, N., Asirvatham, L. G., and Wongwises, S., "Thermoelectric cooling of electronic devices with nanofluid in a multiport minichannel heat exchanger",

Experimental Thermal And Fluid Science, 74: 81–90 (2016).

13. Zhou, S., Sammakia, B. G., White, B., Borgesen, P., and Chen, C., "Multiscale modeling of thermoelectric generators for conversion performance enhancement", ***International Journal Of Heat And Mass Transfer***, 81: 639–645 (2015).

14. Karana, D. R. and Sahoo, R. R., "Effect on TEG performance for waste heat recovery of automobiles using MgO and ZnO nanofluid coolants", ***Case Studies In Thermal Engineering***, 12: 358–364 (2018).

15. Li, Z., Li, W., and Chen, Z., "Performance analysis of thermoelectric based automotive waste heat recovery system with nanofluid coolant", ***Energies***, 10 (10): 1489 (2017).

16. Nnanna, A. G. A., Rutherford, W., Elomar, W., and Sankowski, B., "Assessment of thermoelectric module with nanofluid heat exchanger", ***Applied Thermal Engineering***, 29 (2–3): 491–500 (2009).

17. Mohammadian, S. K. and Zhang, Y., "Analysis of nanofluid effects on thermoelectric cooling by micro-pin-fin heat exchangers", ***Applied Thermal Engineering***, 70 (1): 282–290 (2014).

18. Abdelkareem, M. A., Mahmoud, M. S., Elsaid, K., Sayed, E. T., Wilberforce, T., Al-Murisi, M., Maghrabie, H. M., and Olabi, A. G., "Prospects of thermoelectric generators with nanofluid", ***Thermal Science And Engineering Progress***, 101207 (2022).

19. Atalay, T., Köysal, Y., Özdemir, A. E., and Özbaş, E., "Evaluation of energy efficiency of thermoelectric generator with two-phase thermo-syphon heat pipes and nano-particle fluids", ***International Journal Of Precision Engineering And Manufacturing-Green Technology***, 5 (1): 5–12 (2018).

20. Chang, H., Kao, M.-J., Cho, K.-C., Chen, S.-L., Chu, K.-H., and Chen, C.-C., "Integration of CuO thin films and dye-sensitized solar cells for thermoelectric generators", ***Current Applied Physics***, 11 (4): S19–S22 (2011).

21. Ahammed, N., Asirvatham, L. G., and Wongwises, S., "Entropy generation analysis of graphene–alumina hybrid nanofluid in multiport minichannel heat exchanger coupled with thermoelectric cooler", ***International Journal Of Heat And Mass Transfer***, 103: 1084–1097 (2016).

22. Sundarraj, P., Taylor, R. A., Banerjee, D., Maity, D., and Roy, S. S., "Experimental and theoretical analysis of a hybrid solar thermoelectric generator with forced convection cooling", ***Journal Of Physics D: Applied Physics***, 50 (1): 15501 (2016).

23. Kasireddy, S. and Reddy, V. V., "Thermoelectric Power Generation By Using Solar Parabolic Trough Reflector", 7 (11): 48–54 (2017).

24. Lertsatitthanakorn, C., Jamradloedluk, J., and Rungsiyopas, M., "Electricity

generation from a solar parabolic concentrator coupled to a thermoelectric module", ***Energy Procedia***, 52: 150–158 (2014).

25. Li, K., Garrison, G., Moore, M., Zhu, Y., Liu, C., Horne, R., and Petty, S., "Experimental Study on the Effects of Flow Rate and Temperature on Thermoelectric Power Generation", .

26. ur Rehman, N., Uzair, M., and Siddiqui, M. A., "Optical analysis of a novel collector design for a solar concentrated thermoelectric generator", ***Solar Energy***, 167: 116–124 (2018).

27. Yang, T., Xiao, J., Li, P., Zhai, P., and Zhang, Q., "Simulation and optimization for system integration of a solar thermoelectric device", ***Journal Of Electronic Materials***, 40 (5): 967–973 (2011).

28. Miao, L., Kang, Y. P., Li, C., Tanemura, S., Wan, C. L., Iwamoto, Y., Shen, Y., and Lin, H., "Experimental performance of a solar thermoelectric cogenerator comprising thermoelectric modules and parabolic trough concentrator without evacuated tube", ***Journal Of Electronic Materials***, 44 (6): 1972–1983 (2015).

29. Bjørk, R. and Nielsen, K. K., "The performance of a combined solar photovoltaic (PV) and thermoelectric generator (TEG) system", ***Solar Energy***, 120: 187–194 (2015).

30. Ramkumar, A. and P., S., "Modeling and Simulation of a Line Integrated Parabolic Trough Collector with Inbuilt Thermoelectric Generator", ***I J C T A,*** 10: 589–597 (2017).

31. Li, C., Zhang, M., Miao, L., Zhou, J., Kang, Y. P., Fisher, C. A. J., Ohno, K., Shen, Y., and Lin, H., "Effects of environmental factors on the conversion efficiency of solar thermoelectric co-generators comprising parabola trough collectors and thermoelectric modules without evacuated tubular collector", ***Energy Conversion And Management***, 86: 944–951 (2014).

32. Omer, S. A. and Infield, D. G., "Design and thermal analysis of a two stage solar concentrator for combined heat and thermoelectric power generation", ***Energy Conversion And Management***, 41 (7): 737–756 (2000).

33. Nasrin, R., Rahim, N. A., Fayaz, H., and Hasanuzzaman, M., "Water/MWCNT nanofluid based cooling system of PVT: Experimental and numerical research", ***Renewable Energy***, 121: 286–300 (2018).

34. Contreras, E. M. C., Oliveira, G. A., and Bandarra Filho, E. P., "Experimental analysis of the thermohydraulic performance of graphene and silver nanofluids in automotive cooling systems", ***International Journal Of Heat And Mass Transfer***, 132: 375–387 (2019).

35. Sengers, J. V and Watson, J. T. R., "Improved international formulations for the viscosity and thermal conductivity of water substance", ***Journal Of Physical And Chemical Reference Data***, 15 (4): 1291–1314 (1986).

36. Garnett, J. C. M., "XII. Colours in metal glasses and in metallic films", ***Philosophical Transactions Of The Royal Society Of London. Series A, Containing Papers Of A Mathematical Or Physical Character***, 203 (359–371): 385–420 (1904).

37. Pak, B. C. and Cho, Y. I., "Hydrodynamic and heat transfer study of dispersed fluids with submicron metallic oxide particles", ***Experimental Heat Transfer An International Journal***, 11 (2): 151–170 (1998).

38. Xuan, Y. and Roetzel, W., "Conceptions for heat transfer correlation of nanofluids", ***International Journal Of Heat And Mass Transfer***, 43 (19): 3701–3707 (2000).

39. MAXWELL-GARNETT, J. C., "Colours in metal glasses and in metallic films", ***Phil. Trans. R. Soc. Lond, A***, 203: 385–420 (1904).

40. McAdams 3rd, W. H., "Heat Transmission McGraw-Hill New York", (1954).

41. Tan, L. P., .

42. Zhu, N., Matsuura, T., Suzuki, R., and Tsuchiya, T., "Development of a small solar power generation system based on thermoelectric generator", ***Energy Procedia***, 52: 651–658 (2014).

43. Chen, W.-H., Wang, C.-C., Hung, C.-I., Yang, C.-C., and Juang, R.-C., "Modeling and simulation for the design of thermal-concentrated solar thermoelectric generator", ***Energy***, 64: 287–297 (2014).

44. Chamsa-Ard, W., Brundavanam, S., Fung, C. C., Fawcett, D., and Poinern, G., "Nanofluid types, their synthesis, properties and incorporation in direct solar thermal collectors: A review", ***Nanomaterials***, 7 (6): 131 (2017).

45. Pakdaman, M. F., Akhavan-Behabadi, M. A., and Razi, P., "An experimental investigation on thermo-physical properties and overall performance of MWCNT/heat transfer oil nanofluid flow inside vertical helically coiled tubes", ***Experimental Thermal And Fluid Science***, 40: 103–111 (2012).

46. Phuoc, T. X., Massoudi, M., and Chen, R.-H., "Viscosity and thermal conductivity of nanofluids containing multi-walled carbon nanotubes stabilized by chitosan", ***International Journal Of Thermal Sciences***, 50 (1): 12–18 (2011).

EK AÇIKLAMALAR A.

PROGRAM INPUT DATA

Program

Input data

```
eff= 0.3;% optical efficiency
Ar= 0.0204; % area of receiver m^2
At= 0.5; % area of trough collector m^2
C=18; % concentration ratio
md= 0.013847; % mass flow kg/s
Cp=4187; % heat capacity
Tin=295; % inlet fluid temperature K

Figure of merit parameters
Th=330; % hot side temperature of TEG K
Tc=287; % cold side temperature of TEG K
Aw=0.0165; % area of the cooling system m^2
seg=1; % electric conductivity
k=22; % thermal conductivity of TEG
T=(Th+Tc)/2;% absolute temperature
deltaT=Th-Tc; % temperature difference
ZTm=(S^2*seg/k)*T; % figure of merit
Isol=input('Enter the solar radiation (W/m^2)');
Tamb =input ('Enter the ambient temperature (K)');

Tin=input('Enter the inlet fluid temperature (K)');
Vair= input ('Enter the wind speed (m/s)');
Stefan=5.67*10^-8; % Stefan Boltzmann constant
emiss=0.8; % emissivity

F=0.65; % manufacture of quality factor
n=127; % number of thermocouples
AL=1.96*10^-6; % area of thermo-element m^2
l=1.4*10^-3; % length of thermo-element m
RowTEG=2; % electric resistivity (1/ohm^-1.cm^-1)
Ri=2; % internal resistance of individual cells
Ro=2; % external load resistance
m=5; % number of cells
S=190*10^-6; % Seebeck coefficient v/k
tco=3*10^-3; % thickness of receiver plate(m)
tco1=3*10^-3; % thickness of cooling plate (m)
tteg=4*10^-3,% thickness of TEG (m)
Kco=401; % Thermal Conductivity of Copper Plate W/m.C
Kteg=1; % Thermal conductivity of TEG
Aco=0.0204; % area of receiver plate m^2
Aco1=0.0204; % area of cooling plate m^2
Ateg=16*10^-4; % area of thermoelectric cell m^2
Ai=0.0204; %
R12=tco/(Kco*Aco); % thermal resistance of receiver plate C/W
R34=tco1/(Kco*Aco1); % thermal resistance of cooling plate C/W
Rteg=0.8; % thermal resistance of thermoelectric cell C/W
```

```
Vm=0.165; % flow rate kg/s
V=0.17*10^-3; % volumetric flow rate m3/s
b=0.015; % height of channel m
a=0.05; % width of channel m
Ac=a*b; % cross area m2
Kwater=0.631; % thermal conductivity of water
Vspeed=V/Ac; %speed of fluid m/s
density=992; % density of water kg/m3
vis=0.658*10^-6; % kinematic viscosity m2/s
Dh=2*a*b/(a+b); % hydraulic diameter
Pr=4.32; % Prandtl number of water
Re=Vspeed*Dh/vis; % Reynolds number
L=1;

Tin1=295; % surface temperature of the inlet part of cooling system
Tout1=297.5; % surface temperature of the outlet part of cooling system
Tcave=(Tin1+Tout1)/2; % average surface temperature


if (Re<2300)
   Nu=3.66+((0.065*(Dh/L)*Re*Pr)/(1+0.04*((Dh/L)*Re*Pr)^(2/3)));

else
   Nu=0.023*Re^0.8*Pr^0.3;

end
hi=Nu*Kwater/Dh;

R45=1/(hi*Ai) % thermal resistance for coolant  C/W
Rtot=R12+Rteg+R34+R45 % total thermal resistance C/W

QCfConv=hi*Ac*(Tcave-Tm);

Qin=eff*C*Ar*Isol;
Hair=5.7+3.8*Vair;

effTEG=deltaT*(sqrt(1+Z*Tm)-1)/(Th*sqrt(1+Z*Tm)+(Th/Tc)); % efficiency of
TEG


% calculation of steady state temperature Tr

N=length (Isol);
M=length (md);


for i=1:N
   for j=1:M
```

```
        touT = 0;
    eTeg = 0;
    x0 = 100; % initial point

    while (abs(touT-Tout)>=10^(-4))&&(abs(eTeg-effTEG)>=10^(-4))
      Tm=(Tin+Tout)/2;
      Tcave=Tm;

      g=@(T_r)    (((((eff*Isol(i)*C*Ar)-(Hair*Ar*(T_r-Tamb)+Hair*Aw*(Tcave-
Tamb ))...
        -(Stefan*emiss*Ar*(T_r^4-Tamb^4          )+Stefan*emiss*Aw*(Tcave^4-
Tamb^4)))*(1-effTEG))*Rtot)+Tm)-T_r;

      T_r = fzero(g,x0);

      touT=Tout
      Tout=(((T_r-Tm)/Rtot)/(md(j)*Cp))+Tin;

      Q_d=(T_r-Tm)/Rtot ;

      Th1=T_r-Q_d*R12;

      Tc1=Th1-Q_d*Rteg;
      eTeg=effTEG;


 effTEG=(Th1-Tc1)/Th1*((sqrt(1+Z*(Th1+Tc1)/2)-
1)/(sqrt(1+Z*(Th1+Tc1)/2)+(Tc1/Th1)));

    end

    TR(i,j)=T_r;
    T(i,j)=Tout;
  end
end

TR

Qd=(TR-Tm)/Rtot ;

   Th1=TR-Qd*R12
Tc1=Th1-Qd*Rteg

delT= Th1-Tc1;

Eo=effTEG*delT

Voc=n*m*S*delT
```

```
I=Eo./Voc

for ii=1:length(Isol)
   effth(ii,:)=Qd(ii,:)/(At*Isol(ii)) % thermal efficiency
end
Qteg=F*n*delT.^2*(S/(2*RowTEG))*(AL/l);% output thermoelectric power

Qrconv=Hair*Ar*(TR-Tamb); % convection heat from receiver plate

Qcconv=Hair*Aw*(Tcave-Tamb); % convection heat from cooling pale

Qtcon=Qrconv+Qcconv; % total convection heat transfer

Qrrad=Stefan*emiss*Ar*(TR.^4-Tamb^4); % radiation heat transfer from receiver plate

Qcrad=Stefan*emiss*(Tcave^4-Tamb^4);% radiation heat transfer form cooling plate

Qtrad=Qrrad+Qcrad; % total radiation heat transfer

for i=1:length(md)
Qw(i,:)=md*Cp.*(T(i,:)-Tin);

end

for ii=1:length(Isol)
   effthl(ii,:)=Qw(ii,:)/(Ar*Isol(ii)) % thermal efficiency
end

for jj=1:length(Qin)
Pteg(jj,:)=effTEG*(Qin-Qrconv(jj,:)-Qrrad(jj,:)); % electric power of CTEG
end
for Jj=1:length(Isol)
effELE(Jj,:)=Eo(Jj,:)/(Isol(Jj)*Ar) % electric efficiency
end
```

Result

Appendix Table 1. Result of (I=650, Tamb=27 and Vair=1m/s)

Parameter	Theoretical
Output fluid temperature (℃)	23.2
Hot side thermoelectric temperature Th (℃)	56
Cold side thermoelectric temperature Tc (℃)	26.3
Voltage (V)	2.1
Current (A)	0.23
Power output (W)	0.48
Thermal efficiency (%)	8
Electric efficiency (%)	4.5

Appendix Table 2. Result of (I=720, Tamb=29 and Vair=1m/s).

Parameter	Theoretical
Output fluid temperature (℃)	24.15
Hot side thermoelectric temperature Th (℃)	62
Cold side thermoelectric temperature Tc (℃)	27
Voltage (V)	2.3
Current (A)	0.23
Power output (W)	0.53
Thermal efficiency (%)	9.6
Electric efficiency (%)	4.45

Appendix Table 3. Result of (I=774, Tamb=31 and Vair=1m/s)

Parameter	Theoretical
Output fluid temperature (℃)	24.3
Hot side thermoelectric temperature Th (℃)	66
Cold side thermoelectric temperature Tc (℃)	28.8
Voltage (V)	2.40
Current (A)	0.24
Power output (W)	0.57
Thermal efficiency (%)	7.6
Electric efficiency (%)	4.5

Appendix Table 4. Result of (I=942, Tamb=37.6 and Vair=1m/s)

Parameter	**Theoretical**
Output fluid temperature (℃)	28.2
Hot side thermoelectric temperature Th (℃)	80.5
Cold side thermoelectric temperature Tc (℃)	37.8
Voltage (V)	3.17
Current (A)	0.34
Power output (W)	1.07
Thermal efficiency (%)	11.6
Electric efficiency (%)	6.8

RESUME

Abdalhakim BEN SAOUD completed his primary and Elementary education in Alzawiah, near from the capital of Libya. In 2001, he graduated from Mechanical Engineering Department, Faculty of Engineering, Sirt University. After that, he worked as a mechanical engineering supervising at AL-Zawia University in the period 2002-2008. In 2004, from which he got a scholarship to continue his Msc education. In 2008, he got his MSc degree in Mechanical and Industrial Engineering Department from libyan academy for postgraduate studied. Since 2009, he worked as full-time lecturer in Higher Institute of Industrial Technology at AL-Zawiah. In 2014, he got a scholarship to continue his PhD education in Turkey. He started his PhD academic program at centre of English from Middle East Technical University. He started his PhD academic program at Atilim University,at which he completed the courses and passed the qualification exam. In 2016, He moved to karabuk University, registered in Department of Energy Systems and started his PhD thesis research.